2000

# Scanning electron microscopy of the turtle saccule

Daniel Andrew Bellin
*San Jose State University*

# INFORMATION TO USERS

This manuscript has been reproduced from the microfilm master. UMI films the text directly from the original or copy submitted. Thus, some thesis and dissertation copies are in typewriter face, while others may be from any type of computer printer.

**The quality of this reproduction is dependent upon the quality of the copy submitted.** Broken or indistinct print, colored or poor quality illustrations and photographs, print bleedthrough, substandard margins, and improper alignment can adversely affect reproduction.

In the unlikely event that the author did not send UMI a complete manuscript and there are missing pages, these will be noted. Also, if unauthorized copyright material had to be removed, a note will indicate the deletion.

Oversize materials (e.g., maps, drawings, charts) are reproduced by sectioning the original, beginning at the upper left-hand corner and continuing from left to right in equal sections with small overlaps.

Photographs included in the original manuscript have been reproduced xerographically in this copy. Higher quality 6" x 9" black and white photographic prints are available for any photographs or illustrations appearing in this copy for an additional charge. Contact UMI directly to order.

Bell & Howell Information and Learning
300 North Zeeb Road, Ann Arbor, MI 48106-1346 USA
800-521-0600

UMI®

# SCANNING ELECTRON MICROSCOPY OF THE TURTLE SACCULE

A Thesis Presented to

The Faculty of the Department of Biological Sciences

San José State University

In Partial Fulfillment

of the Requirements for the Degree

Master of Science

by

Daniel Andrew Bellin

May 2000

UMI Number: 1399774





Bell & Howell Information and Learning Company
300 North Zeeb Road
P.O. Box 1346
Ann Arbor, MI 48106-1346

APPROVED FOR THE DEPARTMENT OF BIOLOGICAL SCIENCES

Dr. Michael G. Sneary (Chair)

Dr. Joanne T. Kerr

Dr. Wayne Savage

APPROVED FOR SAN JOSE STATE UNIVERSITY

## ABSTRACT

SCANNING ELECTRON MICROSCOPY OF THE TURTLE SACCULE

By Daniel Andrew Bellin

This study expands the reptilian inner ear database with information derived from scanning electron micrographs of the red-eared turtle saccular macula. Throughout this vestibular sensor three regions were present based on hair cell bundle morphology: striola, extrastriola and periphery. The overlying, otoconial membrane and mass displayed a margin with three zones that corresponded to these underlying regions. Striolar stereovillar bundles were short, wide, unimodal in profile and stereometrically tight. This morphology suggests that the striola may be dynamically sensitive to large acceleratory forces. Extrastriolar stereovillar bundles were taller, narrower, bimodal in profile and stereometrically loose. This morphology suggests that the extrastriola may be dynamically sensitive to small acceleratory forces. Unlike the others, peripheral bundles had a tall, bulbed kinocilium that appeared to be closely linked to the otoconial membrane. Thus, the periphery may function as a tonic sensor, sensitive to positional head changes.

## ACKNOWLEDGEMENTS

This study was undertaken in the neurosensory laboratory of Dr. Michael Sneary at San José State University, and at the Microscope and Graphic Imaging Center ("MAGIC") at California State University, Hayward. Without the fantastic equipment and staff at these labs, this manuscript would not be possible. I would like to thank Dr. Michael Sneary, Dr. Joanne Kerr and Dr. Wayne Savage for their assistance in the preparation of this manuscript as well as for their tutelage throughout my academic pursuits at San José State. Their willingness to provide assistance and insight to my work has truly been invaluable and is forever appreciated. Not only have they greatly contributed to the academic richness of my education, but they have also served as cherished role models in teaching me what it means to be a great educator and a great person. They have provided me with the inspiration and opportunity to pursue my dreams. Lastly, I would like offer my family, friends and Melissa my deepest gratitude for their ongoing love and support.

## TABLE OF CONTENTS

# INTRODUCTION

## *I. Inner Ear Anatomy*

The vertebrate inner ear is composed of a bony labyrinth consisting of a series of spaces and canals within one or more bones of the skull, and an inner membranous labyrinth comprising the sensory organs. These organs are surrounded by a fluid called perilymph and contain a fluid called endolymph. The dorsal aspect of the membranous labyrinth, the *pars superior*, includes the utricle and the posterior, anterior and horizontal semicircular ducts. The ventral aspect, the *pars inferior*, includes the saccule, basilar papilla (Organ of Corti in mammals) and the lagena (absent in mammals, except monotremes). The lagena and basilar papilla comprise the cochlear duct. The sensory neuroepithelium within the ampullae (expanded end) of each semicircular duct is referred to as a crista, while the neuroepithelium within the utricle, saccule and lagena is referred to as a macula. The vestibular apparatus includes the saccule, utricle, the semicircular canals and the lagena. Together they are responsible for one or more of the following functions: coordinating postural muscles and eye movements, establishing positional equilibrium and static orientation of the head in space, detecting linear and angular acceleration of the head in space, or sensing seismic vibrations produced by predators, prey or conspecifics. It is important to note that in different vertebrates, the same end-organ may be utilized to sense different stimuli (1, 2, 3, 4, 5, 6). For example, in some fish, the saccule is utilized as an auditory sensor while in most other vertebrates this organ is vestibular (7, 8, 9, 10).

## *II. Sensory Hair Cells*

### *A. General Features*

The basic organization of sensory hair cells is consistent throughout the vestibular neuroepithelia of vertebrate species studied thus far. Epithelia are comprised of hair cells, supporting cells and nerve fibers and the entire structure rests upon a basement membrane.

Hair cells are commonly described with respect to two main aspects. The apical aspect includes the cuticular plate and the neck region, a somewhat constricted section of the cell just below the plate. The apical aspect faces the endolymphatic space. At this location, the neuroepithelium is sealed by tight junctions that separate the overlying endolymphatic space from spaces in communication with perilymphatic fluids. Endolymph has a high $K^+$ content due to the activity of $Na^+/K^+$-ATPase pumps in nearby secretory cells. Perilymph has a much lower $K^+$ content. The hair cell's apical membrane gives rise to multiple stereovilli and a single kinocilium; this arrangement is known as a hair bundle. Traditionally, the sensory hairs have been called stereocilia. They do not, however, display the characteristic 9 + 2 arrangement of microtubules found in cilia, but instead are packed with actin filaments that should define them as microvilli. For this reason, the present study will use the terminology of Manley (11) and refer to these structures as stereovilli. The kinocilium is a true cilium as described above. Adjacent supporting cells, within the neuroepithelium, create a microvillous brush border circumscribing the perimeter of each hair cell's apical surface. The basolateral aspect of each hair cell begins below the neck region and may surround the widest portion of the

cell. Adjacent supporting cells and afferent and efferent nerve fibers are in synaptic contact with this surface.

Higher vertebrates, especially amniotes, have evolved a special hair cell called the type I hair cell. These flask-shaped cells have a particularly constricted neck region and a flared basolateral aspect. The cell's basolateral surface is completely encompassed by a nerve cup, or calyx. These cells are predominantly found in the central region of the macula but may be located elsewhere (12, 13). The other type of hair cell, type II, typically displays significant variation with respect to shape, cytology, ultrastructure, and bundle morphology (14). In general, they are cylindrical in shape and are innervated by bouton nerve endings. Type II cells typically populate the peripheral region of the macula but may also be found in the center. This is especially true of fish and amphibians since they do not have type I cells (13, 15, 16). Type I and II hair cell distributions and morphologies vary amongst different species. These variations have been associated with the different functions assigned to hair cells and hair cell populations (12, 13, 14).

The cuticular plate lies just beneath the apical surface of the cell. It consists of a thick and rigid network of actin, fimbrin, α-actinin, myosin and tropomyosin filaments (12, 13, 17, 18, 19). Where the actin filament arrays are anti-parallel, they associate with myosin and α-actinin in sarcomere-type arrangements. As a result, the cuticular plate can move in response to changes in the cell's membrane potential, as might be caused by efferent nerve fiber activity. Such movements have been shown to tilt the plate of mammalian type I hair cells, thereby slightly displacing the stereovilli from their normal

position and adjusting the cell's responsiveness (19). In other portions of the cuticular plate, *parallel* arrays of actin filaments reinforce the structural integrity of stereovilli. The cuticular plate of type I cells is several times as thick as in type II cells (12, 13, 17). The plate functions as an anchor for the stereovilli and kinocilia while exerting control over the physical compliance and elasticity of the bundle. Thus, the cuticular plate can directly influence the cell's mechanical responsiveness to stimuli (12, 13, 17, 18).

*B. Stereovilli and Kinocilium Composition and Properties*

Each stereovillus is comprised of thousands of actin filaments that are arranged with unidirectional polarity and cross-linked to increase rigidity (17, 18). These crossbridges are symmetrical, occur at regular intervals along the filaments, and allow the stereovilli to respond to mechanical displacement like inflexible rods (17, 18). Tropomyosin is specifically located at the stereovillar rootlets. These rootlets consist of actin filaments running from the core of each stereovillus into the cuticular plate below. They act as stabilizers. Each stereovillus is of uniform width throughout its length, except at its basal end, where it tapers off as it joins the cuticular plate (17). Stereovilli pivot about this tapered end.

The largest apical projection is called a kinocilium and is a true cilium, with nine pairs of $\alpha$- and $\beta$-tubulin microtubules around the circumference and one pair in the center (20). This nonmotile kinocilium has a greater diameter than the stereovilli and, in some hair cells, has a bulbous tip.

Saccular hair cell bundles are comprised of 40 to 100 stereovilli and a single kinocilium projecting into the endolymphatic space above (5). The kinocilium is eccentrically located at the periphery of the stereovillar bundle. This arrangement defines morphological and functional axes for the bundle. The first (*longitudinal*) axis runs through the bundle towards the kinocilium and the second (*transverse*) axis is perpendicular to the first. The stereovilli are arranged in rows of increasing height along one or both axes. The height profile created by the stereovillar rows within each bundle can vary substantially. Bundles that have a constant slope from the shortest to the tallest rows are referred to as *unimodal.* Other bundles, referred to as *bimodal,* have a change in their slope such that the stepwise progression in height of the shorter stereovillar rows is less than the stepwise progression of the taller rows (12, 13, 21, 22). Specific differences exist with respect to stereovillar number, kinociliary and stereovillar heights and widths, and the presence or absence and prominence of a kinociliary bulb. These differences have been noted throughout the vertebrates (21).

Using the frog saccule as a model, Howard and Ashmore (23) found bundle stiffness to be constant over displacements of 1 μm, and angular deflections of up to ± 0.13 radians, in both directions along the longitudinal axis. This was independent of whether the bundle was being compressed or tensed. Their calculations show bundle stiffness ($k$) to be inversely proportional to the square of the height ($h$) above the cuticular plate where a force is applied to the bundle and directly proportional to the number of stereovilli ($N$):

$$k = \kappa h^{-2} = N\kappa_s h^{-2}$$

where $\kappa_s$ is the pivotal stiffness per stereovillus. Their calculations estimate $\kappa_s$ to be 0.49 $\pm$ 0.15 x $10^{-15}$ N•m•rad$^{-1}$, making the mean pivotal stiffness of the frog saccular hair bundle 22.1 $\pm$ 2.4 x $10^{-15}$ N•m•rad$^{-1}$ and $k$ equal to 256 $\pm$ 28 pN per µm of bundle deflection.

In the kinocilium, the microtubules are not coupled in a particularly tight manner. As a result, the kinocilium contributes minimal stiffness to the bundle, approximately equivalent to that of three stereovilli 10 µm tall. Therefore, the number and length of stereovilli are important determinants of bundle function. These elements are a prominent subject of this research.

*C. Stereovillar Interconnections*

Filamentous interconnections link stereovilli and coordinate their movements, which occur about an axis that is very close to the cuticular plate (24). These interconnections are part of a glycocalyx, a negatively charged cell membrane coating that contains glycoconjugates. This glycocalyx causes the stereovilli to repel each other (21, 23). Thus, both "static" mechanical and "dynamic" electrical forces reinforce the bundle's geometrical array.

There are three varieties of stereovillar connections. Horizontal *shaft connections* run the entire length of each stereovillus, connecting it to its neighbors. The horizontal shaft connections are very thin, approximately 6 nm in width (21). Incident forces on hair cell bundles are fairly evenly translated from the kinocilium to all the stereovilli via these filamentous links (23). *Tip-link connections* couple the beveled tip of each

stereovillus to the shaft of its neighbor in the next tallest row (5, 21, 25). Although stereovilli are separated by 50-100 nm at the tips, the tip-links allow for shear movement of up to 200 nm. This is possible because the links attach to the core of the taller stereovillus and, in response to displacement, bend it from the center and displace the plasma membrane (23). There are also *stereo-kinociliar bonds* that connect several of the tallest stereovilli to the kinocilium. These bonds have two components: 1) macromolecular, extracellular filaments, and 2) intracellular filaments bound to the plasma membrane within the kinocilium (26).

*D. Bundle Stereometrics*

Two main stereovillar arrangements, or bundle stereometrics, have been documented. In one, the stereovilli in transverse rows are closely associated. These are known as *straight* rows and the bundles are designated as *tight* (21, 22). Tight bundles may diminish the force vector by a factor of cosine 30°, due to the fact that all of their tip-links are aligned at a 30° angle from the longitudinal axis. Thus, tight bundles may have a unique directional sensitivity (21).

In other bundles, the stereovilli in transverse rows are not closely associated. These are known as *staggered* rows and the bundles are designated as *loose* (21, 22). In loose bundles, each stereovillus has a link to its neighbors one order of magnitude taller and shorter in the same longitudinal row. As a result, the stereovilli of transverse rows are interspersed by those in longitudinal rows. Loose bundles have twice as many rows as do tight bundles, although they have the same number of stereovilli. Since every other

transverse row is connected to another in loose bundles, two different populations of stereovilli are created within each bundle. Bagger-Sjöbäck and Takumida (21) suggest that shaft connections are required to keep the loose bundle moving as a unit.

### *III. Macular Dimensions: Comparative Issues*

The sensory epithelium of the saccule has a shape that varies almost as much as the nature of the vertebrates in which it appears. However, there are some anatomical characteristics common to all. For example, vertebrate saccular maculae consistently lie in a parasagittal plane, with the macular surface and bundles facing laterally. Thus, the stereovilli in the right macula point laterally to the right, and vice versa for the left macula.

The location of the kinocilium and therefore the direction of bundle morphological polarization define the functional polarization, or orientation, of each hair cell. Hair cells are often grouped into populations based on this polarization, such that a single macula can have multiple hair cell populations. For instance, hair cells are typically divided into two populations whose orientations are approximately 180° in opposition across a central dividing line. Surrounding this central division is a region called the *striola*, often dominated by type I cells with morphologically similar bundles (14). This region is characteristic of higher vertebrates, including mammals. Additional populations of hair cells, based upon bundle morphology, are observed as one proceeds away from the striola towards more peripheral regions of the epithelium.

*A. Fish*

The fish saccule is generally long and narrow, measuring about 1 mm long and 200 μm wide, with its longer side lying in the rostro-caudal direction. It is common for the macula in these animals to be wider at the anterior end and to bend slightly in the dorsal direction. The fish saccule consistently displays the most complex hair cell polarization patterns among vertebrates, with taxonomically distinct species often displaying similar bundle orientations. Fish usually have four or more discrete bundle orientation patterns within a singular saccular maculae (9, 10).

The lemon shark, a cartilaginous fish, differs in several aspects from other fish. First, it has a U-shaped saccule, with an additional curve in the posterior arm. It is much larger, approximately 9.5 mm long and 1 mm wide. In addition, the macula bends upon itself, effectively changing spatial planes, such that the anterior extension faces posteriorly while the posterior arm faces laterally. Finally, there are only two bundle orientation patterns, with hair cells polarized perpendicular to, and away from, the midline (27).

The bichir has a J-shaped macula, most of which extends antero-dorsally, except the epithelium does not twist upon itself as it does in the shark. In this case, the macula is limited to one plane. It is approximately 1.5 mm long and 130 μm wide. Like the shark and unlike other fish, it has only two bundle orientation patterns on either side of a midline. These patterns follow along the length of the macula (9).

*B. Amphibians*

The amphibian saccular macula also lies in the parasagittal plane. In salamanders and newts, the macula is oblong in shape and is approximately 400 μm wide and 500 μm long. Its longer, vertical axis is slightly tilted posteriorly. In the bullfrog it is similarly shaped, but the vertical axis is slightly tilted anteriorly. Moreover, the plane of the macula is tilted, such that the ventral margin extends laterally and the dorsal margin extends medially. The amphibian macula has two hair cell populations, both of which are polarized away from a U-shaped midline (28, 29).

*C. Reptiles*

Jorgensen (30) reported that the turtle macula is a long, narrow, sensory epithelium extending along half of the antero-ventral border of the saccule. It is less than 2 mm long and is approximately 300 μm wide throughout, with a slight widening at the ventral end. Jorgensen also reported the presence of a central striolar region that follows the shape of the macula. He stated that type I cells were arranged into two "irregular zones" that ran parallel to and on either edge of the striola. Jorgensen did not report hair cell numbers or densities within the reptilian saccular macula.

*D. Birds*

The avian saccular macula is unique in that it lies in the coronal plane. It is elliptically shaped, with its long axis along the medial-lateral axis. An S-shaped dividing line, running medio-laterally, separates the two hair cell populations. Bundles are

polarized away from the midline. In addition, there is a large population of type I cells occupying the region ventral to the midline (31).

*E. Mammals*

The saccular macula of guinea pigs, cats, and monkeys has an L-shape, with the longer leg running along the anterior-posterior axis and pointing in a postero-ventral direction. It is about 2 mm long. The other leg is about 1 mm long and is at 90° angle to the longer extension. An L-shaped central striola divides the two hair cell populations. The human saccule is shaped like an elongated kidney bean, with its anterior portion lying more superior that its posterior portion. Its mean length is 2.60 mm and its mean width is 1.43 mm. When viewed from above, it is evident that the macular surface is in three dimensions (22, 32). The human saccule also has a striolar region (17, 32, 33).

***IV. Stereovillar Bundles: Comparative Issues***

Classification of hair cell populations in the saccular macula is often based upon bundle morphology. Various descriptors have been created such as types F1 to F3 and types A to D. This bewildering nomenclature has not been standardized. Cells have been further categorized by their shape and pattern of afferent innervation. It is only in recent studies of mammals that type I and II cells have been associated with specific bundle morphologies, however these findings are not all in agreement (21, 22, 34, 35). The height of an individual bundle is usually indicated by the height of the tallest stereovilli.

*A. Fish*

As mentioned above, the fish saccule may take on a number of functions. In cases where the saccule is an auditory sensor, the diverse polarities of hair cell populations are thought to provide information concerning the directionality of sound. (7, 20, 36).

There are three main types of teleost bundle morphologies, all of which contain 40 to 70 stereovilli, that are consistently found in specific macular locations (7, 8, 9, 10, 36). *F1* bundles, which are centrally located and are the most numerous, have a kinocilium that is up to 2 μm tall and may be twice the height of the tallest stereovilli (7, 8, 9, 10, 36). They are surrounded by several rows of *F3* in the extrastriolar region. The F3 cells are similar to F1, except that the bundle is somewhat taller. Up to five rows of *F2* cells are located at the extreme macular periphery. Their kinociliary heights range from 4 to 6 μm, while their tallest stereovilli are 0.5 to 1.0 μm tall (7, 8, 9, 10, 36).

In comparison to teleosts, the deep-sea fishes have maculae dominated by the F3 bundle type. However, they do display the multiple bundle orientation patterns, found in many shallow water fish (8).

*B. Amphibians*

Up to six types of type II hair cells have been identified, based on bundle morphology, in the bullfrog otoconial sensory epithelia (28, 29). All of the bundles in the bullfrog saccule are polarized away from the striolar midline. A separate morphology, known as *type D*, is predominant in the saccular striola. Each type D bundle has a bulbed

kinocilium that equals the height of the tallest stereovilli. These cells may be responsible for the vibrational sensitivity of the frog saccule (6, 28, 29, 37). Lateral to the type D bundles are *type A* bundles. Each type A bundle also has a bulbed kinocilium but it is about twice as tall as the tallest stereovilli. Type A bundles are probably involved in auditory and gravistatic sensitivity (6, 28, 29). The extreme periphery of the bullfrog macula has a sparse population of cells with very short stereovilli and an unbulbed kinocilium that is several times taller than the tallest stereovilli. Thus, there is a gradual increase in height and a change in bundle morphology, moving from the center to the periphery (6, 28).

*C. Birds*

There is evidence that the avian saccule is a vestibular sensor (31, 38). Type I cells show significant homogeneity within and between avian end-organs (12, 13). Type I cells are generally located in the central region of the macula. In the pigeon, type I hair cell bundles are 16.3 ± 0.5 μm tall (12, 13) and, in the rhea, are 5 to 7 μm tall (38).

Type II hair cells, though also found in the central region, are mainly at the periphery of the macula. They vary considerably with respect to cell width and length, cell surface area, neck length and width, bundle height, area and stereovillar population density. Type II cell bundles are taller than type I, measuring 19.8 ± 0.8 μm in the pigeon (13) and 20-30 μm in the rhea (38). The macula has approximately equal numbers of unimodal and bimodal bundles, which are equally distributed amongst type I and II cells. Bimodal bundles are taller than unimodal bundles (12, 13).

*D. Mammals*

The mammalian saccule is a detector of gravity and linear acceleration (17, 22, 32, 33, 39, 40).

Type I mammalian cells are typically found in the striolar region and have bundles whose stereovilli are tall and equivalent in height to the kinocilium (34, 35). In the guinea pig, a popular model for mammalian study, type I cell bundles increase in height from the striolar region, where they are about 8 μm tall, to the peripheral region, where they are about 11 μm tall (22). One report indicates that type I bundles have a 2:1 loose to tight bundle stereometric ratio (21), while other studies show an approximately equal distribution and frequency of loose and tight stereometrics (22).

Type II cells are generally associated with the peripheral regions of the macula. They have a tall kinocilium whose height is a multiple of the tallest stereovilli (34, 35). Type II hair cell bundles in the guinea pig, however, are located throughout the macula and show a consistent height of 4.5 μm (22). As with type I bundles, some studies show that type II bundles have a 2:1 loose to tight bundle stereometric ratio (21), while others indicate an equal distribution and frequency of loose and tight stereometrics (22).

Studies of human type I cell bundles show approximately 70 stereovilli per bundle, whereas type II cell bundles have approximately 50 stereovilli. As with other mammals, human type I cell bundles seem to be taller than type II cell bundles (17).

## *V. Otoconial Membrane and Mass: Comparative Issues*

The saccule, lagena and utricle each contain a mass above the macula. In fish, this mass is a single structure and is called an otolith. In other vertebrates, this mass consists of an acellular gelatinous membrane that encases a slurry of secreted calcium carbonate crystals. Changes in the inertia of the otoconial mass, due to gravity and linear acceleration, cause it to displace and distort the underlying bundles. Previous studies have described various degrees of connectivity between the otoconial membrane and hair cell bundles (5, 6).

### *A. Fish*

The teleost saccular otolith has a species-specific shape and typically fills 75% of the saccular chamber (7, 41). The otolithic membrane connects the otolith to the sensory epithelia and covers the entire macula. There are numerous sockets into which the hair cell bundles project. These cavities are irregularly shaped and represent fluid or gel-filled spaces in which hair cell bundles move. All bundles are adjacent to the same margin of the socket such that they display a similar off-center placement (41). The shape of these sockets limits the movement of bundles to their direction of polarization (7, 10, 41).

The teleost otolithic membrane is a viscoelastic matrix of glycoproteins. The membrane has an upper *gelatinous layer* and a lower filamentous *subcupular layer* (42). The former is furthest above the bundles, while the latter interfaces with the bundles. Its structural proteins, including saccular collagen, are produced by secretory cells that are located along the periphery of the macula (42).

*B. Amphibians*

The otoconial membrane of the bullfrog consists of three separate layers. The outer layer, or *otoconial layer*, contains the calcium carbonate crystals and is robust (Note: despite its name, this layer is on the innermost surface of the otoconial membrane). Stereovilli project through the thin, acellular *inner layer*. The *intermediate layer* lies between the inner and outer layers. In contrast to the utricle and lagena, known sensors of linear acceleratory forces, the intermediate layer in the bullfrog saccule is thick and is physically linked to the underlying stereovilli. This relationship is thought to aid in the detection of seismic vibrations (6, 43).

*C. Mammals*

The mammalian otoconial membrane also has a layered arrangement. The innermost *otoconial layer* of the membrane thickens to make a ridge above the striolar region of the macula. The *gelatinous layer*, which is very fibrous, forms a seal over the sensory epithelium, separating it from non-sensory areas. Above the striola, the membrane contains numerous perforations, or sockets, that accommodate the underlying striolar bundles (34, 35).

The gelatinous layer is further subdivided into three layers. The *upper layer* is in contact with the otoconia. The *honeycomb layer* is poorly developed in the striolar region and is more substantial in the extrastriolar regions, where stereovillar bundles insert into its chambers. The *meshwork layer* is dome-shaped and houses the stereovillar

bundles. It fastens the base of the honeycomb layer to the supporting cells. In the peripheral zones, stereovilli are associated most closely with the meshwork layer (34, 35).

In the striola, where bundles are generally shorter, there is a space that contains a very diminished meshwork layer. Thus, striolar bundles are presumably freestanding, or less tightly coupled to the overlying mass. It has, therefore, been asserted that the striola is a specialized region for the reception of dynamic signals whereas the peripheral regions, where bundles are more tightly coupled, are probably involved in the reception of static signals (3, 34).

### *VI. Innervation*

Three classes of afferent nerve fibers in mammalian vestibular maculae have been described. *Calyx units* are found only in the striolar region. Their thick fibers give rise to single calyces that encase the basolateral surface of one to several adjacent type I cells (15, 16). *Bouton units* are found mainly in the peripheral and extrastriolar zones. Their thin fibers often contact several type II hair cells. *Dimorphic units* make up the most numerous type of nerve fibers, found in all regions of the neuroepithelium of mammals, innervating both type I and II cells. They are medium sized fibers that terminate as both thick calyces and thin collaterals. They provide innervation to most of the peripheral type I cells, the striolar type II cells, and to both the type I and II cells in the extrastriolar zone (5, 16).

Three subclasses of calyceal endings have been described based on their varied myelination characteristics. Among these are the unmyelinated *U-type* and the partially myelinated *M/U-type*, both of which form unmyelinated collateral processes that terminate presynaptically and postsynaptically on type I and II cell neurons (12, 15). Moreover, the macula, including those of mammals and reptiles, displays *gap junctions* between hair cells and supporting cells. These gap junctions are thought to provide a low-resistance pathway for electrical coupling between cells (44). Such findings reinforce the idea that the higher vertebrate macula contains a microcircuitry network that allows for the preprocessing of sensory information, positive- and negative-feedback loops, and the enhancement of signal detection (12, 15, 16, 39, 44, 45, 46).

*Hair Cell Type Considerations*

Type I cell-neuron complexes are characterized by fast conduction velocity, high sensitivity and broad operating ranges that are modulated by an intracellular second messenger system. They display irregular spontaneous activity and produce transient, adaptive responses to constant stimulation. The implication is that type I hair cell-nerve complexes, in correlation to freestanding bundles, provide phasic responses to changes in head velocity due to gravity or linear acceleration (5, 6, 14, 22). In contrast, type II cell neurons are characterized by low conduction velocity and low sensitivity to mechanical stimuli. They have regular spontaneous activity and show tonic responses to constant stimuli. In conjunction with the observation that longer, peripheral bundles are often linked to the otoconial membrane, type II cell-nerve complexes probably provide tonic

responses to changes in head velocity due to gravity or linear acceleration (5, 6, 14, 22, 35).

It is important to note that studies have correlated macular location with the electrophysiological properties of hair cell-nerve complexes (14, 17, 43, 47).

### *VII. Mechano-electrical Transduction*

A variety of mechanical stimuli may displace the overlying otoconial mass. When the bundle is displaced, the stereovilli pivot at their point of insertion into the cuticular plate. At the distal tip of each stereovillus is a mechanically sensitive ion channel, which initiates the mechano-electrical transduction process. At present, evidence indicates that when the bundle is displaced toward the kinocilium, tip-links pull on the channels and open them. Potassium ions flow through the plasma membrane of the stereovilli and the hair cell membrane depolarizes. Voltage-gated $Ca^{2+}$ channels, located in the basolateral membrane, react to the increased membrane potential and allow an influx of $Ca^{2+}$. As a result, synaptic vesicles located at points along the basolateral membrane release neurotransmitter onto afferent neurons (5, 17, 25). Finally, $Ca^{2+}$-dependent-$K^+$ channels, also in the basolateral membrane, provide outward rectifying $K^+$ currents that allow the excess $K^+$ to flow into the perilymph. The cell, thus, repolarizes. When the bundle is deflected away from the kinocilium, the mechano-channels in the stereovilli close, causing hyperpolarization of the hair cell. Lateral bundle deflection causes no change in membrane potential (14, 17, 21, 25, 34, 48, 49).

Mechano-electric transduction results from the amount of bundle displacement. The number, length and arrangement of stereovilli are therefore important in determining a cell's sensitivity (18, 25, 50). Although stereovilli do not react like perfectly rigid beams, the force applied is essentially proportional to their displacement. Any nonlinear displacement-receptor potential characteristics exhibited during mechano-electric transduction in saccular hair cells are likely due to the properties of ion channels or alterations in cuticular plate tension (18, 23).

Interestingly, hair cells are known to exhibit *electro-mechanical* transduction. In this instance, changes in the cell's membrane potential cause a displacement of the bundle (See above section II.A.)

### *VIII. Study Significance*

The saccule has many important functions. Wilson et al. (40) reports that the mammalian saccule contributes to vestibulospinal reflexes and therefore plays a role in postural muscle coordination. Other studies report that the saccule plays a role in spatial orientation, communication and predator evasion (6). Curthoys' (51) research in non-human vertebrates implicates the saccule in eye movement reflexes. Kigma's (52) work in humans also correlates saccular stimulation with eye torsion and the statolith-ocular reflex. The study of Guyot and Vibert (53) in pediatric patients with Mondini dysplasia, a condition in which the pars superior is absent and all that remains of the inner ear is a functional saccule, shows that the saccule provides enough information to allow for

walking. This reinforces the precept that the human saccule makes a major contribution to vestibular function.

A better insight into the correlation of morphology and function in the saccule will allow for an improved understanding and treatment of inner ear pathologies. One such pathology, waltzing syndrome, has been studied in the guinea pig. This animal was shown to suffer from vestibular dysfunction caused by genetically induced degeneration of vestibular hair cells, including stereovillar fusion (54).

The present study uses scanning electron microscopy to further define the structure of sensory hair cells within the turtle saccular macula. It focuses on bundle morphology since previous research has linked this aspect to mechano-electrical responsiveness. This will help to better define the saccule's function. In addition, since bundle morphology seems to vary within and between end organs, it would be helpful to understand the contribution of specific hair cell populations to overall saccular function.

Despite its limitations, the present study also seeks to help decipher whether a correlation exists between hair cell type and bundle morphology, in view of previous vertebrate studies having reached contradictory conclusions. Moreover, it is important to be able to accurately define and distinguish between type I and II hair cell morphologies, since research is striving to decipher their functions by classifying their morphological, mechano-electrical and electrophysiological properties. Finally, the information provided in this study will serve as a morphological basis for a subsequent set of functional studies.

# MATERIALS AND METHODS

The Institutional Animal Care and Use Committee of San José State University approved the animal use protocol employed in this research (#650).

## *I. Dissection and Fixation*

Fifteen red-eared turtles, *Chrysemys scripta elegans,* were used in the present study. All animals were adult in size. An areflexic anesthesia was induced via hypothermia in the turtles. This was done via refrigeration of the animals for one hour and then placing the animals in an ice water bath for approximately one-half hour.

The turtles were decapitated and the large temporal muscles were cut to expose the dorsal surface of the skull. The skull was opened along the midline, exposing the dorsal and caudal portions of the brain. The brain tissue was removed, and the thin medial walls of both otic capsules were opened. The otic capsules were flushed with fixative (0.5% acrolein, 1.0% paraformaldehyde, 3.0% glutaraldehyde, in a 0.1M $Na^{+}$-cacodylate buffer) as dissection proceeded and the entire head was placed in fixative for 24 hours.

Each membranous labyrinth was then carefully dissected free of the surrounding otic capsule and placed in fresh fixative, which was refreshed each day for 48 hours. The white saccular otoconial mass was removed from the membranous labyrinth at this point (before decalcification) and air-dried.

### *II. Decalcification and Post-fixation*

To decalcify the remaining otoconia for scanning electron microscopy, each membranous labyrinth was placed in a fresh solution of 3.0% glutaraldehyde, with 0.1M EDTA (ethylenediaminetetraacetic acid) in a 0.1M $Na^+$-cacodylate buffer. Tissue vials were then placed on a rotator during the day and refrigerated overnight. The solution was replaced daily until the otoconia were judged to be completely decalcified, as indicated by visual inspection. This typically took 3-5 days.

The tissues were post-fixed and stained in 1% osmium tetroxide ($OsO_4$). This procedure made the otoconial membrane brittle and therefore more easily removed from the macular surface. The tissues were placed on ice and exposed to the stain for 3-4 hours. Next, the tissues were carefully rinsed in a 0.1M solution of $Na^+$-cacodylate buffer for 2-3 minutes.

### *III. Dehydration and Critical-point Drying*

The tissues were then dehydrated in a graded series of ethanols during which they were lightly agitated. The dehydration schedule was as follows: 70% alcohol solution for 3 minutes, 80% alcohol solution for 3 minutes, 95% alcohol solution for 3 minutes, twice, and finally 100% alcohol solution for 3 minutes, twice.

The tissues were then immediately critical-point dried using a DCP-1 Critical Point Drying Apparatus (Denton Vacuum, Inc.). The $CO_2$ (g) pressure was leveled-off at 1650 psi., where it was stabilized for 3 minutes. The pressure was then decreased to 800 psi., at a rate of 100 psi./min., and then further decreased from 200 psi./min. to 0 psi. In

the literature, tissue shrinkage of approximately 20% is assumed from the fixation, dehydration and critical-point drying protocols (55). The values reported in this study are not corrected for shrinkage.

### *IV. Sputter-coating and SEM*

The tissues were mounted on metal stubs using Colloidal Silver Paste (Ted Pella, Inc.). At this time, a final tissue dissection was performed. The tissues were oriented so the macula faced upward, at various angles. A low-pressure blower was used to remove remaining otoconia and other debris with minimal tissue trauma. Fissures in the maculae were created by delicate manipulation of the tissue with the dissection instruments. In some cases, a fine metal probe or eyelash attached to a stick was placed beneath the macula and forced upwards to create a clean fissure. Attempts to slice downwards through the epithelium often resulted in smeared or compressed tissue.

The specimens were sputter-coated with 350 Å of palladium-gold using a Hummer II Sputter-coater (Technics, Inc.) at the following settings:

Amperage: 10 milliamps;

Pressure: 110 millitorr;

Voltage: 9 volts;

Duration: 3'40".

The above process was repeated for 15 animals, producing a total of 30 saccular specimens.

The specimens were viewed with an XL40 Scanning Electron Microscope (Philips Electronics, Inc.) at the Microscope and Graphic Imaging Center ("MAGIC") located at California State University, Hayward. The following instrument settings were used:

Working distance: 3-4 mm at 10,000 (+) magnification, 5-6 mm at 5,000-10,000 magnification, and 7-8 mm at 0-5,000 magnification;

Spot size: 3 at 10,000 (+) magnification, 4 at 5,000-10,000 magnification, and 5 at 0-5,000 magnification;

Acceleration voltage: 10.0 kV at 0-12,000 magnification; 15.0 kV for high resolution at 12,000 (+) magnification.

The Philips XL40 digital images were captured on a ZIP disc, using a ZIP drive (Iomega Corp.), for transfer to San José State University. Images were processed on a Power Macintosh 9600/223 (Apple Computer, Inc.), using PhotoShop 4.0.1 software (Adobe Systems, Inc.), at the Neurosensory Laboratory of San José State University.

### *V. Morphological Analysis*

Electron micrographs of macular surfaces and hair cells were visually analyzed for macular dimensions, bundle morphology and hair cell type. Measurements of macular dimensions, cell bodies and bundles were acquired by using both the Philips XL40 electron microscopy software and by measuring the printed images themselves.

By comparing the NBR (ratio of neck width to body width) and NPR (ratio of neck width to cuticular plate width) ratios of hair cells, Ricci et al. (13) developed a

method to distinguish between macular hair cells that is 90% accurate and applicable to many species. This technique was used in the present study to more accurately identify hair cell types.

To be acceptable for analysis, hair cells and bundles had to be clean and undamaged by tissue processing. In addition, the bundle had to be erect. To be stereometrically described, the bundles also had to be viewed face-on.

### *VI. Statistical Analysis*

All values for macular and cellular dimensions are expressed as mean values ± standard deviation.

# RESULTS

## *I. Saccular Macula*

The turtle saccular macula was J-shaped and oriented in a parasagittal plane. The macular surface generally faced laterally (Figures 1, 2). It had a main body, located at the ventral margin of the saccular space, and an elongated arm that extended 180° antero-dorsally along the edge of the space. The main body had a mean length of 435 ± 57 μm and a mean width of 293 ± 69 μm, while the arm had a mean width of 107 ± 25 μm and a mean length of 1,483 ± 155 μm (n = 16). The body was kidney bean-shaped and had a concave, dorsal margin and a convex, ventral margin. Approximately 50 hair cells spanned the short axis (width) of the body. The entire surface of the body was curved (curved laterally) and contained about 1,000 hair cells. The arm was considerably more narrow, with approximately 20 hair cells across its width. Its surface did not remain in the parasagittal plane, but twisted so that its most anterior portion faced posteriorly and was in the coronal plane, while its most dorsal portion faced ventrally and was in the horizontal plane.

The present study defined three macular regions: 1) a central striola, 2) two adjacent extrastriolar regions, and 3) two outside, or peripheral, regions. All three of these regions appeared to run the entire length of the macula. The striolar region of the macula extended on either side of the midline (Figure 3). Throughout the entire macula, the striolar region was approximately 80 μm wide and displayed approximately 10 hair cells across the short axis. The extrastriolar regions, which were adjacent to the striolar region, narrowed as they extended from the body, where they were approximately 50 μm

wide and contained 7 hair cells across, to the arm, where they were approximately 20 μm wide and contained 2 hair cells across. The peripheral regions, which were adjacent to the extrastriolar regions, also narrowed from the body, where they were approximately 100 μm wide and displayed 8 hair cells across, to the arm, where they were approximately 40 μm wide and displayed 3 hair cells across.

There was no apparent regularity in the spacing of hair cell bundles within the epithelium. While some groups of hair cells had their apical margins in contact, the majority of hair cells were surrounded by the apices of supporting cells. The latter feature was noted most often in the peripheral regions implying a slight increase in hair cell density towards the center of the macula.

### *II. Bundle Morphology*

*General Trends*

From the striola to the extrastriola, there was an increase in stereovillar height, followed by a decrease in height and count per bundle in the periphery. Kinociliary heights, on the other hand, showed a dramatic increase in height from the striola to the periphery of the macula. All bundles appeared to have one kinocilium such that they were polarized perpendicular to, and away from, a central midline (Figure 4).

Throughout the entire macular body and arm there was a significant correlation between bundle morphology and macular location. Thus, three bundle types were categorized: striolar, extrastriolar and peripheral (indicated as A, B, and C in Figures 5, 6, 7, 8, 9).

*A. Striolar Bundles*

Hair cell bundles in the striola had 66.9 ± 6.0 stereovilli comprising 17 rows. Half the bundles had staggered and half had straight rows (n = 27) (Figures 8, 9). The face of each striolar bundle was triangular, with rows tapering from 9 to 4 stereovilli across and displayed an unbulbed kinocilium not taller than the tallest stereovilli, at 4.77 ± 0.62 μm (n = 26) (Figures 9, 10). An approximately linear, or unimodal, height gradation was displayed from the shortest to the tallest stereovillar rows. In addition, the striola displayed a minimum of otoconial remnants and no evidence of a connection to the overlying otoconial membrane (Figures 11, 12).

*B. Extrastriolar Bundles*

Extrastriolar bundles had 66.9 ± 8.5 stereovilli comprising 16 rows with a mix of bundles with staggered and straight rows (n = 27) (Figures 8, 9). Extrastriolar bundles had a distinct and intermediate rectangular bundle face morphology, with rows tapering from 8 to 5 stereovilli, and an unbulbed kinocilium that extended slightly above the tallest stereovilli, at 6.86 ± 0.75 μm versus 6.18 ± 0.97 μm, respectively (n = 9) (Figures 9, 13). Bundles in this region showed some variation. The extrastriolar bundles that were more peripherally located showed a gradual increase in kinociliary and stereovillar height and greater amounts of otoconial remnants, indicating some connectivity to the otoconial membrane. A non-linear, or bimodal, height gradation was formed by the

sequence of stereovillar rows, the tallest rows with a slightly greater slope (Figures 14, 15).

*C. Peripheral Bundles*

Peripheral bundles had 37.4 ± 5.2 stereovilli comprising 10 rows (n = 27) (Figures 8, 9). Each kinocilium, often tipped with a small but distinct bulb, was double the length of the tallest stereovilli, at 8.21 ± 1.17 μm and 3.87 ± 0.76 μm, respectively (n = 11) (Figures 9, 16). Peripheral bundles showed the greatest degree of variation. Bundles furthest from the midline showed an increase in kinociliary height and a concurrent decrease in both the height and number of stereovilli. Peripheral regions were consistently covered with significant debris, indicating a link to the overlying otoconial membrane (Figures 17, 18, 19).

***III. Bundle Stereometrics***

Of the striolar bundles that were acceptable for analysis, 9 had straight stereovillar rows and were tight bundles, and 8 had staggered stereovillar rows and were loose, resulting in an approximate 1:1 ratio of loose to tight bundles (21, 22). The tight bundles had an average of 10.2 ± 1.0 rows, and the loose bundles had an average of 18.4 ± 2.3 rows (n = 26) (Figures 9, 20).

Of the extrastriolar bundles that were acceptable for analysis, 2 had straight stereovillar rows and could be classified as tight bundles, and 7 had staggered stereovillar rows and could be classified as loose, resulting in an approximate 3.5:1 ratio of loose to

tight bundles (21, 22). The tight bundles had an average of 9.5 ± 0.7 rows, and the loose bundles had an average of 19.7 ± 1.8 rows (n = 9) (Figures 9, 21).

Of the peripheral bundles that were acceptable for analysis, 5 had staggered stereovillar rows and could be classified as loose (21, 28), such that all peripheral bundles could be classified as loose. The loose bundles had an average of 10.0 ± 1.2 rows (n = 11) (Figure 9).

It is important to note that the present study limited its stereometric descriptions to bundles that were erect, clean and could be viewed face-on.

### *IV. Stereovilli*

Along their main shaft, stereovilli did not significantly vary with respect to width, regardless of location within the macula. At their base, where they interfaced with the cuticular plate, stereovilli tapered by about one-third. Striolar bundle stereovilli were 166 ± 0.06 nm wide (n = 35), and extrastriolar bundle stereovilli were 152 ± 0.5 nm wide (n = 11). No peripheral stereovilli were acceptable for width analysis. Stereovilli tapered to an approximate width of 100 nm just above the cuticular plate. Striolar bundle kinocilia were 225 ± 0.00 nm wide (n = 4). Kinocilia from the other regions were not acceptable for width analysis.

### *V. Cell Type*

The mean NPR of several flask shaped cells in the present study was 0.57 ± 0.09 while the mean NBR was 0.35 ± 0.12 (n = 8). The fact that they had constricted neck

regions, flared basal regions and remnants of what might have been neural calyces suggests the presence of type I cells in the striolar region of the turtle saccule (Figure 22).

Most other cells within the striola had the columnar appearance of type II cells. Fissures showed either cells or spaces where the apex of the cells had non-constricted neck regions. The mean NPR of several of these cells was $0.77 \pm 0.17$ while the mean NBR was $0.74 \pm 0.15$ ($n = 8$). These data suggest the presence of type II hair cells in the striola (Figure 23). Regardless of body shape, however, all hair cells in the striolar region displayed consistent bundle morphology, as previously described. Unfortunately, no accurate data was acquired from fissures that would allow analysis of hair cell bodies in either the extrastriolar or peripheral regions.

### *VI. Otoconial Membrane and Mass*

The otoconial mass consisted of a main portion that occupied the majority of the saccular space and an extension that covered the macular body (Figure 24). The mass consisted of crystals immersed in a meshwork and was entirely encased in an otoconial membrane (the specimens in the present study were mostly free of this membrane) (Figures 25, 26). The margin of the mass was textured and revealed a trizonal arrangement, when viewed at higher magnification. These zone widths corresponded approximately to the widths of the striolar and extrastriolar/peripheral zones, combined (Figure 26). The width of the striolar zone was approximately 80 μm throughout, while the extrastriolar/peripheral zones ranged from approximately 150 μm to 80 μm. In addition, the striolar zone of the otoconial mass contained numerous sockets. These

sockets appeared to lie over the striolar region of the macula and *in vivo* would associate with the striolar bundles (Figure 27).

Similar sockets were found in what might be the otoconial membrane. In one specimen, this membrane was observed *in situ* lying over the striolar region of the macula (Figure 28).

# DISCUSSION

## *I. Saccular Macula*

The present study complements and expands upon the findings of Jorgensen (30) in the turtle by dividing the macula into two segments: a main body and an extended arm. Both of these were found to be larger than previously reported. Specifically, the body was found to be wider and more kidney-bean shaped, and the arm was found to extend much farther, about 180° in the antero-dorsal direction. It is important to note that Jorgensen studied the *Testudo graeca* and the *Chrysemys scripta elegans* turtles, while the present study investigated only the latter.

The shape of the turtle saccular macula seems to be unique among vertebrates. Nevertheless, the macula of the bichir fish and the lemon shark do bear some resemblance to the turtle's in overall shape and bundle orientation patterns.

## *II. Bundle Morphology*

### *General Trends*

The bundle height trends in the turtle saccule, as seen in the present study, are generally mimicked in other vertebrates, including fish (7, 9, 10, 36), amphibians (6, 28), birds (31), and mammals (34, 35). However, in each case, significant differences exist. The fish macula displays differences in bundle orientation patterns (7, 20, 36), while the avian macula does not seem to have the long, bulbed kinocilia as seen in the turtle (12, 13). Amphibian maculae have striolar bundles with prominently bulbed kinocilia

suggesting a strong connection to the otoconial membrane (6, 28). Mammalian bundles have an increase, not a decrease, in peripheral stereovillar heights (22).

The data presented here define three different bundle morphologies based on hair cell macular location: striolar, extrastriolar and peripheral.

*A. Striolar Bundles*

The relative heights of the striolar bundles seen in the present study resemble those of other species' striolar, or centrally-located, bundles, including those of the rhea, human and most closely those of the guinea pig. Lapeyre et al. (22) found that guinea pig type I hair cell bundles with short, triangular bundles in the striola were the least sensitive to displacement and, along with their afferent fibers, were putatively phasic, adaptive sensors to linear acceleration. Given the morphological similarities, turtle striolar hair cells may have a similar function.

There are three main morphological findings of the present study that suggest striolar bundles are the stiffest, and least sensitive to displacement, among those in the turtle macula. First, striolar bundles were the shortest and widest, and contained as many stereovilli as other bundles (See Figures 8, 9, 11). The findings of Ricci et al. (12, 13) and Howard and Ashmore (23) assert that shorter, wider bundles are stiffer, since stiffness is linearly proportional to the number of stereovilli and is inversely proportional to the square of the height above the cell at which point the force is administered.

Second, the striolar region had the greatest concentration of tight bundles, which are theoretically more rigid than loose bundles (21).

Third, the shortest three rows of stereovilli were of very similar height, forming a small shelf at the base of the bundle (See Figures 10, 12). This was not observed in extrastriolar or peripheral bundles. DiCaprio and Peterson (56) described similar bundles morphologies in type I hair cells in the semicircular canal of turtles. They found these bundles were not only wider, with more numerous and shorter stereovilli, but also had a gentler slope and a triangular bundle face. While the functional significance of this organization is unclear, there are some possibilities. Based on the bundle dynamics defined by Howard and Ashmore (23), the stereovillar rows at the foot of striolar bundles may augment their stiffness and thereby increase the magnitude of the force needed for bundle displacement. Such stiffness would also decrease the time it takes for the bundle to return to its neutral position. This could allow for faster hair cell repolarization.

The above findings add merit to the hypothesis that striolar bundle-afferent neuron complexes are dynamic sensors that provide transient, afferent sensory input regarding linear acceleration. Moreover, these findings potentially differentiate the functions of striolar versus extrastriolar bundles. Given that extrastriolar bundles are taller and do not seem to have the same shelf, they may be easier to depolarize and, thus, provide greater sensitivity to velocity changes. Small accelerations or decelerations may be sufficient to stimulate the extrastriolar hair cells, while larger changes may be required to stimulate striolar hair cells.

*B. Extrastriolar Bundles*

The second tier of stereovillar rows that created the bimodal profile in extrastiolar bundles may contribute to their mechanical properties (12). Based on the findings of Howard and Ashmore (23), the taller rows would require less force to move and, consequently, would make the extrastriolar bundle more susceptible to displacement and, therefore, more sensitive. In addition, the variable structure of these bundles may be indicative of variable function in this hair cell population (12, 13).

There is further evidence that would suggest a heightened sensitivity in extrastriolar hair cells. Weng and Correia (49) found that the presence of rectifying currents in vestibular type II cells is correlated with fast activation kinetics: time-to-peak-current times, activation times and repolarization times. Eighty-six percent of pigeon extrastiolar type II cells with rectifying outward currents were fast, while 100% of striolar type II cells lacked these currents and had slow activation kinetics. Also, rectifying inward $K^+$-currents were found 1.6 times more often within the extrastiolar zone, versus the striola. Thus, if the extrastriolar cells of the turtle are type II, one would expect them to exhibit sensitive, dynamic and adaptive responses to stimuli. As a result, the properties and therefore functions of extrastriolar bundles may supplement those in the striola.

*C. Peripheral Bundles*

Tall kinocilia and short, small bundles, as seen in the peripheral regions of the present study, have also been reported in the bullfrog. These bundles were implicated in

vibrational sensitivity (8, 28, 37, 57). However, the more substantial connections required for such sensitivity are not found in the turtle. As a result, these hair cells probably do not have such a function.

Jorgensen and Christensen (38) also found tall bundles in the peripheral region of the common rhea. No functional information is available for the rhea.

The excess otoconial membrane debris found on the kinocilia of peripheral bundles indicates some connection to the overlying mass. Thus, these hair cell bundles, in contrast to those in the striola and extrastriola, may provide static, non-adaptive sensory input to constant linear forces.

### *III. Bundle Stereometrics*

The present study found an overall 2:1 ratio of loose to tight bundles. However, the greatest concentration of tight bundles was clearly in the striolar region. In contrast, the findings of Bagger-Sjöbäck and Takumida (21) in the guinea pig show a constant loose-to-tight ratio of 2:1 throughout the striolar, extrastriolar and peripheral regions, as well as amongst type I (equally tall stereovilli and kinocilium) and type II (short stereovilli, tall kinocilium) bundles.

Amongst the 162 type I and II cells that Lapeyre et al. (22) analyzed, about 50% had tight bundles and about 25% had loose bundles. The distribution of tight and loose type I bundles was roughly equivalent in all zones. In contrast, tight type II bundles decreased from the striola (41%) to periphery (15%) while loose type II bundles increased from striola (12%) to periphery (39%). Such findings may explain the lower

numbers of tight bundles in extrastriolar and peripheral region observed in the turtle. Specifically, there may be an increase in the number of type II bundles towards the periphery of the macula (discussed below).

Bagger-Sjöbäck and Takumida (21) found that tight bundles had about half the stereovillar rows than did the loose bundles, at 9 to 11 and 18 to 22, respectively. Such findings were confirmed in the present study which shows no significant difference in overall stereovillar count amongst tight and loose bundles. Bagger-Sjöbäck and Takumida also discussed how tight and loose bundle stereometrics might affect bundle sensitivity and responsiveness. In light of those findings and the findings in the present study, the functionality of turtle saccular hair cells could differ between the striolar, extrastriolar or peripheral macular regions.

*IV. Stereovilli*

Stereovilli in the present study were of uniform diameter throughout the macula. Nevertheless, the stereovillar count was significantly greater in the striolar and extrastriolar regions than in the peripheral region. In contrast, other studies have found type I cell-stereovilli significantly thicker than type II cell-stereovilli (17, 21). Thicker stereovilli might modulate bundle stiffness and further diversify bundle sensitivity. Diversity of stereovillar diameter has been observed only in mammals.

*V. Cell Type*

In conjunction with morphological analysis, the present study found type I cells in the striolar region. Their NPR (0.57 ± 0.09) and NBR (0.35 ± 0.12) values were comparable to those of type I cells reported by Ricci et al. (13) (NPR 0.55 ± 0.02, NBR 0.37 ± 0.01). The present study also found type II cells in the striola. Their NPR (0.77 ± 0.17) and NBR (0.74 ± 0.15) values were comparable to type II cells reported by Ricci et al. (NPR 0.99 ± 0.02, NBR 0.63 ± 0.01). However, due to the present study's limited data, it is not possible to speculate on the relative frequency of these cells.

Reinforcing the assertion that type I hair cells exist in the striola was the frequent observation that the apical margins of several striolar hair cells were in close contact. This could indicate a grouping of type I cells innervated by a single calyx (16).

Since there is a mix of hair cell types in the striola, despite a highly conserved bundle morphology, both types may function similarly. Chabbert's (58) findings in the bullfrog saccule, connecting the location of type II hair cells to morphology and electrophysiological character, support this hypothesis. He proposed that three kinds of type II cells exist: 1) peripheral elongated hair cells (PEHCs), 2) central cylindrical hair cells (CCHCs), and 3) central flask-shaped hair cells (CFHCs). Based on the differences in their $I_{Ca}$ (voltage activated calcium current) and $I_{Kca}$ ($Ca^{2+}$-activated potassium current), Chabbert hypothesized CFHCs as having different functions than CCHCs since these two cell types were sensitive to different frequencies. In light of the fact that the present study showed a mix of cell body shapes in the striolar region, it seems quite possible that

centrally located type II cell-neuron complexes function similarly to neighboring type I cell-neuron complexes.

Previous studies suggest that type I cells are primarily located in the center of the macula, with a general decrease in their numbers, along with an increase in the numbers of type II cells, towards the periphery of the macula (17, 21, 22, 38). While the present study was unable to produce fissures of extrastriolar and peripheral regions, the observed trends in bundle morphology may be partially explained by this.

Zahm's (46) findings in the reptilian saccule were validated in the present study. Zahm found that adjacent lizard hair cells were separated by the supranuclear aspect of a supporting cell monolayer interposed between the hair cells. In addition, Zahm found that hair cells were innervated by a mix of bouton and calyceal nerve endings, implying a mix of type I and II hair cells. He made no specific mention of the exact location and ratio of these two types, however. The present study also provides evidence that type I and II cells are located in the striolar region. As a result, among vertebrates, reptiles appear to have evolved a relatively complex vestibular sensor. In addition, based on neurophysiological studies of the microcircuitry of type I cells, they may preprocess the information derived from these hair cells (14, 15, 16, 45). Other evidence in the turtle supports the concept of a complex peripheral sensory epithelium (59).

Unlike the findings of Jorgensen (30) it was not apparent that type I cells were present in two distinct parallel, parastriolar zones. It should be noted that the present study was limited to the relatively few fissures that provided conclusive cell body information.

Lapeyre et al. (22) described extrastriolar hair cells in the guinea pig whose bundles resemble those in the present study and that fit the traditional description of type II hair cells. Given this similarity and the findings of Jorgensen (30), the extrastriolar cells of the turtle might be type II cells.

The findings of Bagger-Sjöbäck and Takumida (21) in the guinea pig described type I cells as having a bimodal bundle slope, in both tight and loose stereometric arrangements. Type II cells were found to have a unimodal slope, also in either a tight or loose arrangement. While the present study did find some striolar bundles that displayed a slightly bimodal slope, it was unable to correlate such a slope to either a specific cell type or stereometric arrangement. The present study suggests that bundle morphology is associated more with location than cell type.

### *VI. Otoconial Membrane and Mass*

Striolar bundles may have a relationship with the sockets of the outer layer of the turtle's otoconial membrane. However, the present study found no evidence for a physical connection. These sockets may help promote movement of the bundles in a particular direction and, thus, promote directional selectivity (7, 10, 41).

Since the sockets in the otoconial membrane were limited to a region that was approximately the width of the striola, it did not appear that the extrastriolar bundles were associated with sockets. However, the otoconial mass did reveal a depression that ran the length of the macula and was approximately the width of both the extrastriolar and

peripheral regions. The functional significance of this is not clear, except that an association between these bundles and the otoconial membrane and mass is suggested.

### *VII. Putative Function*

It is difficult to correlate the present study's morphological findings to function since no data on turtle macular function are available. Still, some possibilities exist and can be used to construct testable hypotheses for functional studies.

Given the predatory behavior of the lemon shark and the unique dynamics of its three-dimensional aquatic environment, a U-shaped macula with a multifaceted planar orientation may have evolved as an adaptation to predatory life. Although there are obvious differences in the behavior and environments of the shark and red-eared turtle, they are both predators that need to maneuver quickly in the water in response to the movements of their prey. These common needs may partially explain the evolution of the shape of their maculae.

As in the turtle, Popper (9) found that hair cells in the central region of the bichir macula had kinocilia that were closer in height to the tallest stereovilli, whereas in the periphery, the kinocilia were more than twice the height of the stereovilli. Popper argued that the J-shape of the macula is the result of functional evolution, but he is unclear exactly what influenced this development. Despite the differences in the saccular macula of the bichir versus other fish, Popper concluded that it is still a likely sensor of sound. This is not probable in the case of the turtle saccule as the basilar papilla is the auditory sensor (60).

Type A bundles in the bullfrog saccule have a bulbed kinocilium with a strong physical link to the overlying otoconial membrane. These cells provide for seismic sensitivity (6, 28, 29, 37). As cells in the turtle saccule lack bundles with prominent kinociliary bulbs, they are most likely not seismically sensitive.

Finally, the data provided by this study suggest that the turtle saccule is a vestibular sensor. The striolar hair cell bundles, probably on type I and II cells, are the stiffest kind and so the least sensitive to displacement. As a result, these may be dynamic sensors of linear acceleratory and gravitational forces. The turtle's extrastriolar bundles, probably on type II cells, may also be dynamic sensors. Given their morphology, they may be more sensitive to the same forces. The peripheral hair cells might be the static receptors of the turtle saccular macula. They displayed some evidence of a connection to the otoconial mass. Similar cells in other vertebrates remain depolarized so long as the otoconial mass is displaced (2, 4, 17, 22, 49). Thus, based on the extent of their deflection, peripheral cells in the turtle may provide information about the constant velocity or acceleration of the head.

Given the polarizations of hair cells and the complex and extensive shape of the turtle saccular macula, it is reasonable that this end-organ provides information on forces not only in the vertical plane but also in the horizontal plane, and potentially other planes. This may aid the animal in its predatory behavior as it negotiates its aquatic and terrestrial habitat.

### *VIII. Study Limitations*

In rats between the ages of three months and two years, Nakayama et al. (61) noted several age-related changes in vestibular hair cells. These included substantial hair cell loss, decreased stereovillar and kinociliar numbers, and greatly increased numbers of microvilli covering the maculae. These microvilli occasionally created a "giant cilia". Although all of the animals used in the present study were adult in size, no information correlating growth and deviation of reptilian inner ear sensors is available. In addition, it is unclear how diet or environment can alter hair cells.

It should also be noted that due to the angles of some of the micrographs, it was not always possible to decisively discern staggered versus straight bundle stereometrics. As a result, some bundles were not stereometrically defined.

## BIBLIOGRAPHY


1. Baird RA. The anatomy of the reptilian ear. In: Gans C, Parsons TS, eds. Biology of the reptilia: morphology. New York: Academic Press, 1970:193-275.

2. Baker J. Supraspinal descending control: the medial postural system. In: Zigmond MJ, Bloom FE, Landis SC, Roberts JL, Squire LR, eds. Fundamental neuroscience. New York: Academic Press, 1999:913-90.

3. Cohen-Salmon M, El-Amraoui A, Leibovici M, Petit C. Otogelin: a glycoprotein specific to the acellular membranes of the inner ear. Proc Natl Acad Sci USA 1997; 94:14450-55.

4. Ganong WF. Hearing and equilibrium. In: Butler JP, Suver AM, Langan C, eds. Review of medical physiology. Stamford, CT: Appleton and Lange, 1997:161-74.

5. Goldberg JM. The vestibular end organs: morphological and physiological diversity of afferents. Cur Op Neurobio 1991; 1:229-35.

6. Lewis ER, Pawley JB. Direct SEM study of frozen inner ear. Scanning 1981; 4:131-40.

7. Popper AN. Comparative scanning electron microscopic investigations of the sensory epithelia in the teleost sacculus and lagena. J Comp Physiol 1981; 200:357-74.

8. Popper AN. Scanning electron microscopic study of the sacculus and lagena in several deep sea fishes. Am J Anat 1980; 157:115-36.

9. Popper AN. Scanning electron microscopic study of the otolithic organs in the bichir (Polypterus bichir) and shovel-nose sturgeon (Scaphirhnchus platorynchus). J Comp Neurol 1978; 181:117-28.

10. Popper AN, Hoxter B. The fine structure of the sacculus and lagena of a teleost fish. Hearing Res 1981; 5:245-63.

11. Manley GA. A review of the auditory physiology of the reptiles. Prog Sens Physiol 1981; 2:49-134.

12. Ricci AJ, Cochran SL, Rennie KJ, Correia MJ. Vestibular type I and type II hair cells. 2: Morphometric comparisons of dissociated pigeon hair cells. J Vestib Res 1997; 7:407-20.

13. Ricci AJ, Rennie KJ, Cochran SL, Kevetter GA, Correia MJ. Vestibular type I and type II hair cells. 1: Identification in the pigeon and gerbil. J Vestib Res 1997; 7:393-406.

14. Eatock RA, Rusch A, Lysakowski A, Saeki M. Hair cells in mammalian utricles. Otolaryngol Head Neck Surg 1998; 119:172-81.

15. Ross MD. Morphological evidence for local microcircuits in rat vestibular maculae. J Comp Neurol 1997; 379:333-46.

16. Ross MD, Rogers C, Donovan K. Innervation patterns in rat saccular macula. Acta Otolaryngol (Stockh) 1986; 102:75-86.

17. Morita I, Komatsuzaki A, Tatsuoka H. The morphological differences of stereovilli and cuticular plates between type I and type II hair cells of human vestibular sensory epithelia. J Otorhinolaryngol Relat Spec 1997; 59:193-97.

18. Slepecky N, Chamberlain S. Immunoelectron microscopic and immunofluorescent localization of cytoskeletal and muscle-like contractile proteins in inner ear sensory hair cells. Hearing Res 1985; 20:245-60.

19. Zenner HP, Zimmermann U. Motile responsiveness of vestibular hair cells following caloric, electrical or chemical stimuli. Acta Otolaryngol (Stockh) 1991; 111:291-97.

20. Lu Z, Popper AN. Morphological polarizations of sensory hair cells in the three otolithic organs of a teleost fish: fluorescent imaging of ciliary bundles. Hearing Res 1998; 126:47-57.

21. Bagger-Sjöbäck D, Takumida M. Geometrical array of the vestibular hair bundle. Acta Otolaryngol (Stockh) 1988; 106:393-403.

22. Lapeyre P, Guilhaume A, Cazals Y. Differences in hair bundles associated with type I and II vestibular hair cells of the guinea pig saccule. Acta Otolaryngol (Stockh) 1992; 112:635-42.

23. Howard J, Ashmore JF. Stiffness of sensory hair bundles in the sacculus of the frog. Hearing Res 1986; 23:93-104.

24. Osborne MP, Comis S, Pickels J. Morphology and cross-linkage of stereovilli in the guinea pig labyrinth examined without the use of osmium as a fixative. Cell Tissue Res 1984; 237:43-48.

25. Hudspeth AJ. How the ear's works work. Nature 1989; 341:397-404.

26. Ernstson S, Smith CA. Stereo-kinociliar bonds in mammalian vestibular organs. Acta Otolaryngol (Stockh) 1986; 101:395-402.

27. Corwin JT. Postembryonic production and aging inner ear hair cells in sharks. J Comp Neurol 1981; 201:541-53.

28. Lewis ER, Li C. Hair cell types and distributions in the otolithic and auditory organs of the bullfrog. Brain Res 1975; 83:35-50.

29. Lewis ER, Li C. Evidence concerning the morphogenesis of saccular receptors in the bullfrog (Rana catesbeiana). J Morph 1973; 139:351-62.

30. Jorgensen JM. The sensory epithelia of the inner ear of two turtles, Testudo graeca L. and Pseudemys scripta (Schoepf). Acta Zool (Stockh) 1974; 55:289-98.

31. Jorgensen JM, Andersen T. On the structure of the avian maculae. Acta Zool (Stockh) 1973; 54:121-30.

32. Sun J, Fang Y, Jiang S. Scanning electron microscope observation of human vestibular sensory epithelia. Chung Hua Erh Pi Yen Hou Ko Tsa Chih 1995; 30:326-28.

33. Takagi A, Sando I. Computer-aided three-dimensional reconstruction and measurement of the vestibular end-organs. Otolaryngol Head Neck Surg 1988; 98:195-202.

34. Lim DJ. Fine morphology of the otoconial membrane and its relationship to the sensory epithelium. Scan Electron Microsc 1979; 3:929-38.

35. Lim DJ. Morphological and physiological correlates in cochlear and vestibular sensory epithelia. Scan Electron Microsc 1976; 2:269-76.

36. Platt C, Popper AN. Variations in lengths of ciliary bundles on hair cells along the macula of the sacculus in two species of teleost fishes. Scan Electron Microsc 1984; 4:1915-24.

37. Xiaolong Y, Lewis E, Feld D. Seismic and auditory tuning curves from bullfrog saccular and amphibian papillar axons. J Comp Physiol A 1991; 169:241-48.

38. Jorgensen JM, Christensen JT. The inner ear of the common rhea (Rhea americana). Brain Behav Evol 1989; 34:273-80.

39. Uchino Y, Sato H, Suwa H. Excitatory and inhibitory inputs from saccular afferents to single vestibular neurons in the cat. J Neurophysiol 1997; 78:2186-92.

40. Wilson VJ, Gacek RR, Maeda M, Uchino Y. Saccular and utricular input to cat neck motoneurons. J Neurophysiol 1977; 40:63-73.

41. Steinacker A, Menton DN, Romero A. Toadfish saccular hair cell bundle has a preferred orientation in the otolithic membrane. Hearing Res 1990; 48:145-49.

42. Davis JG, Burns FR, Navaratnam D, Lee AM, Ichimiya S, Oberholtzer JC, Greene MI. Identification of a structural constant and one possible site of postembryonic formation of a teleost otolithic membrane. Proc Natl Acad Sci USA 1997; 94:707-12.

43. Baird IL. Comparative transduction mechanisms of hair cells in the bullfrog utriculus. 1: Responses to intracellular current. J Neurophysiol 1994; 71:666-83.

44. Hama K. Fine structure of the afferent synapse and gap junctions on the sensory hair cell in the saccular macula of goldfish: a freeze-fracture study. J Neurocyt 1980; 9:845-60.

45. Chimento TC, Ross MD. Evidence of a sensory processing unit in the mammalian macula. Ann NY Acad Sci 1996; 781:198-212.

46. Zahm DS. Gap junctions between sensory and supporting cells of the utricular and saccular maculae in Anolis carolinensis examined by transmission electron microscopy. Am J Anat 1980; 158:263-73.

47. Sugihara I, Furukawa T. Morphological and functional aspects of two different types of hair cells in the goldfish sacculus. J Neurophysiol 1989; 62:1330-43.

48. Hackney CM, Fettiplace R, Furness DN. Functional morphology of stereociliary bundles on turtle cochlear hair cells. Hearing Res 1993; 69:163-75.

49. Weng T, Correia MJ. Regional distribution of ionic currents and membrane voltage responses of type II hair cells in the vestibular neuroepithelium. J Neurophysiol 1999; 82:2451-61.

50. Crawford AC, Fettiplace R. The mechanical properties of ciliary bundles of turtle cochlear hair cells. J Physiol 1985; 364:359-79.

51. Curthoys IS. Eye movements produced by utricular and saccular stimulation. Aviat Space Environ Med 1987; 58:A192-97.

52. Kingma H. Clinical testing of the statolith-ocular reflex. J Otorhinolaryngol Relat Spec 1997; 59:198-208.

53. Guyot JP, Vibert D. Patients with charge association: a model to study saccular function in the human. Ann Otol Rhino Laryngol 1999; 108:151-55.

54. Sobin A, Weraall J. A morphological study of vestibular sensory epithelia in a strain of the waltzing guinea pig. Acta Otolaryngol (Stockh) 1983; Suppl 396:1-32.

55. Bozzola JJ, Russell LD. Specimen preparation for scanning electron microscopy. In: McKean BL, ed. Electron microscopy: principles and techniques for biologists. Sudbury, MA: Jones and Bartlett, 1999:49-71.

56. DiCaprio L, Peterson EJ. Differences in hair bundle size of type I and type II ampullary receptors in a turtle. In: Popelka GR, ed. Abstracts of the 15th annual midwinter research meeting of the Association for Research in Otolaryngology. St. Petersburg Beach, FL: Assoc Res Otolaryngol, 1992:15-24.

57. Christensen-Dalsgaarad J, Jorgensen MB. The response characteristics of vibration-sensitive saccular fibers in the grassfrog, Rana temporaria. J Comp Physiol A 1988; 162:633-38.

58. Chabbert CH. Heterogeneity of hair cells in the bullfrog sacculus. Pflügers Arch-Eur J Physiol 1997; 435:82-90.

59. Sneary MG, Bhide K, Lee L. Electron microscopy of the turtle saccular and lagenar sensory epithelia. In: Popelka GR, ed. Abstracts of the 19th annual midwinter research meeting of the Association for Research in Otolaryngology. St. Petersburg Beach, FL: Assoc Res Otolaryngol, 1996:174.

60. Sneary MG. Auditory receptor of the red-eared turtle: 1. General ultrastructure. J Comp Neurol 1988; 276:573-87.

61. Nakayama M, Helfert RH, Konrad HR, Caspary DM. Scanning electron microscopic evaluation of age-related changes in the rat vestibular epithelium. Otolaryngol Head Neck Surg 1994; 111:799-806.

# APPENDIX: FIGURES

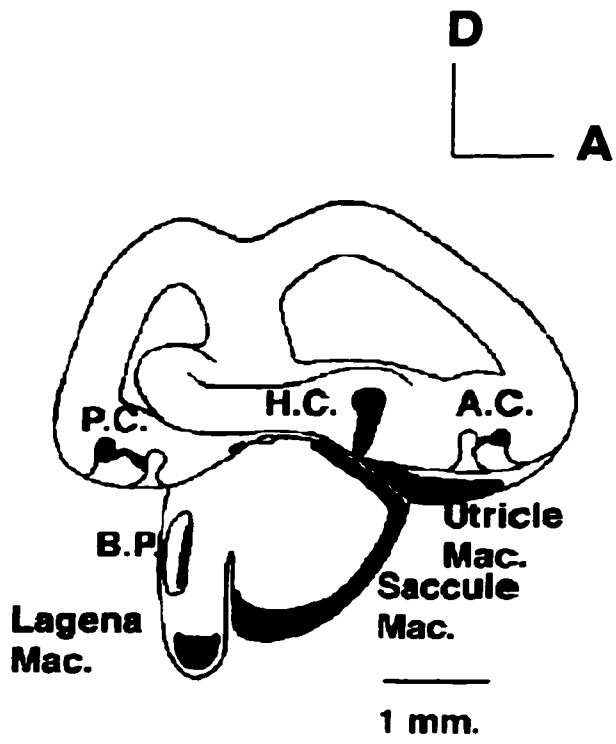


FIGURE 1. A schematic diagram representing a lateral view of the right membranous labyrinth in the turtle [PC = posterior semicircular canal, AC = anterior semicircular canal, HC = horizontal semicircular canal, Mac. = macula, A = anterior, D = dorsal; modified from Sneary (50)].


FIGURE 2. Lateral view of the left saccule revealing the main body and arm regions of the macula as they lie in the parasagittal plane. The region of the saccule that contains the major portion of the otoconial mass is also shown (*). The otoconial mass and membrane have been removed (45x).

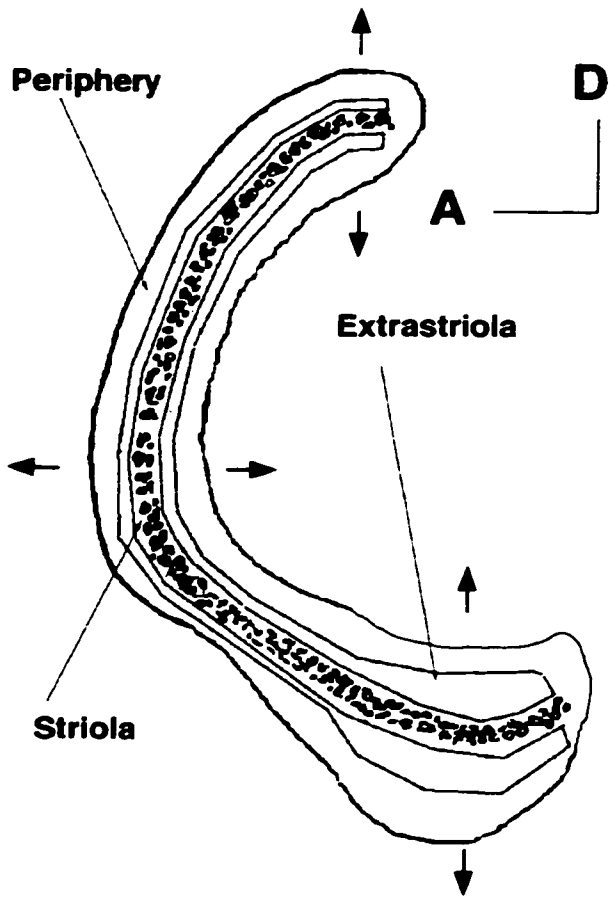


FIGURE 3. Schematic diagram of the saccular macula showing the central striolar region as well as the extrastriolar and peripheral regions, running parallel on both sides of the striola. The larger arrows, pointing perpendicular and away from the striola, indicate the polarization of hair cells on either side of the striolar dividing line (A = anterior, D = dorsal).

FIGURE 4. View of the striolar region and the central macular dividing line. On either side of the line, bundles are oppositely polarized, as indicated by the line and arrows. Note the uniform morphology of the bundles and the lack of otoconial debris (3358x).

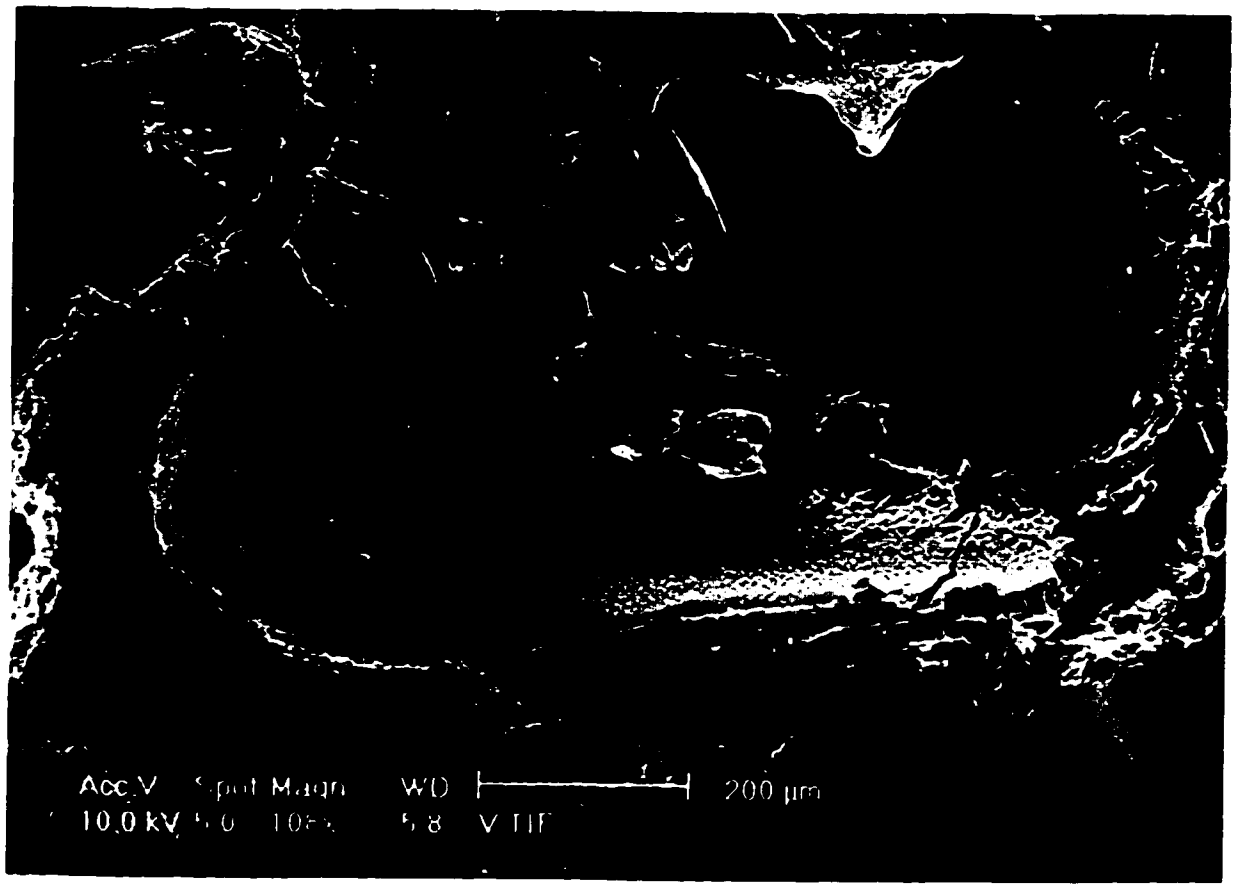


FIGURE 5. Lateral view of the right labyrinth showing the regions within the body of the macula that correspond to specific bundle morphologies: striolar (A), extrastriolar (B), and peripheral (C). These regions are also present in this arrangement within the macular arm (108x).

FIGURE 6. View of the macular body showing the transition in hair cell bundle morphology occuring between the striolar (A), extrastriolar (B) and peripheral (C) regions. The lines indicate this division. Note that the otoconial remnants appear to increase towards the periphery of the macula (1468x).

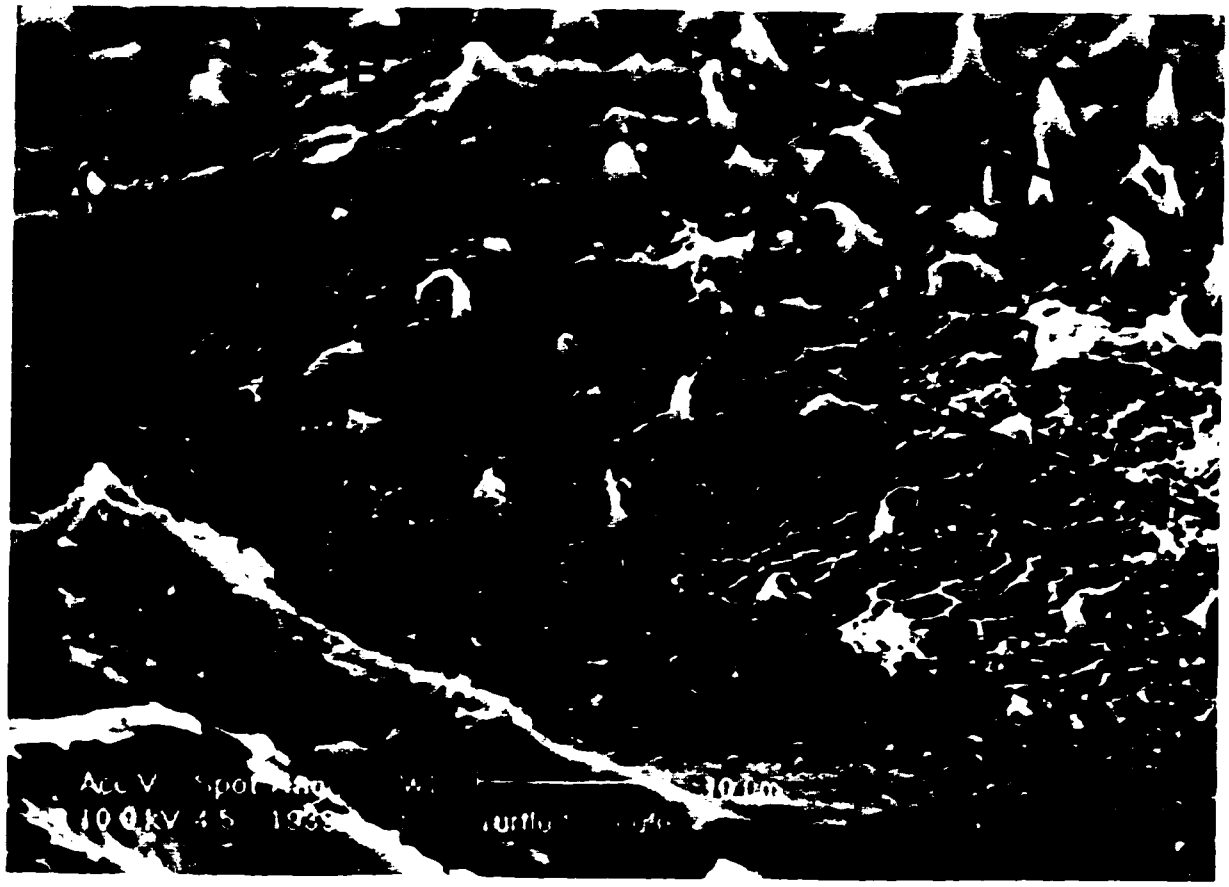

FIGURE 7. View of the macular arm showing the transition in hair cell bundle morphology occuring between the striolar (A), extrastriolar (B) and peripheral (C) regions. The lines indicate this division (1939x).

FIGURE 8. Number of stereovilli in hair cell bundles from the striolar, extrastriolar, and and peripheral macular regions (n = 27). Values are mean +/- standard deviation.

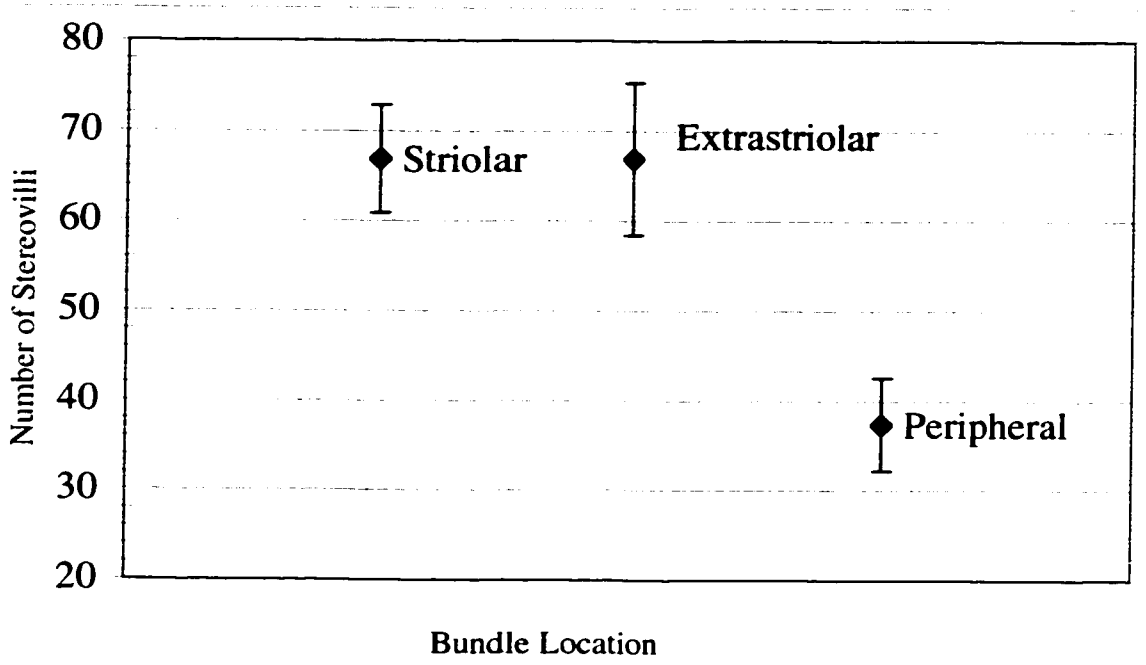

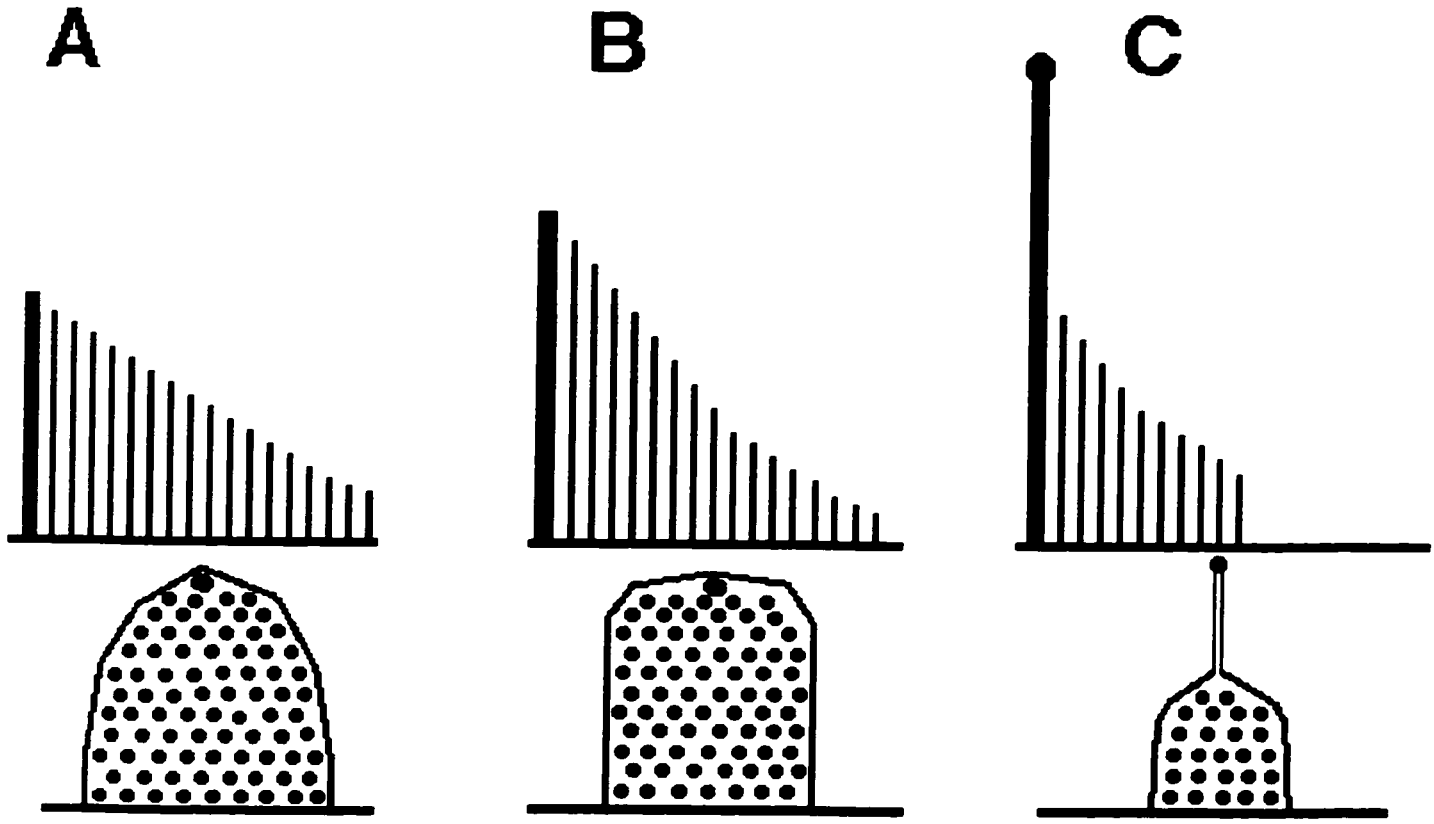


FIGURE 9. Schematic diagrams of the three bundle types: striolar (A), extrastriolar (B), and peripheral (C). The top diagrams show bundle profiles indicating the relative heights and number of stereovillar rows. The thick lines indicate kinocilia. The peripheral bundle has a bulbed kinocilium. The bottom diagrams show the relative shape of bundle faces and the number of stereovilli per row. The dots indicate the tips of stereovilli. The large dots indicate kinocilia. The striolar and extrastriolar bundle faces have been drawn with staggered rows, in loose configurations.

FIGURE 10. Kinociliar and stereovillar row numbers and heights in striolar bundles (n = 26). Values are mean +/- standard deviation.

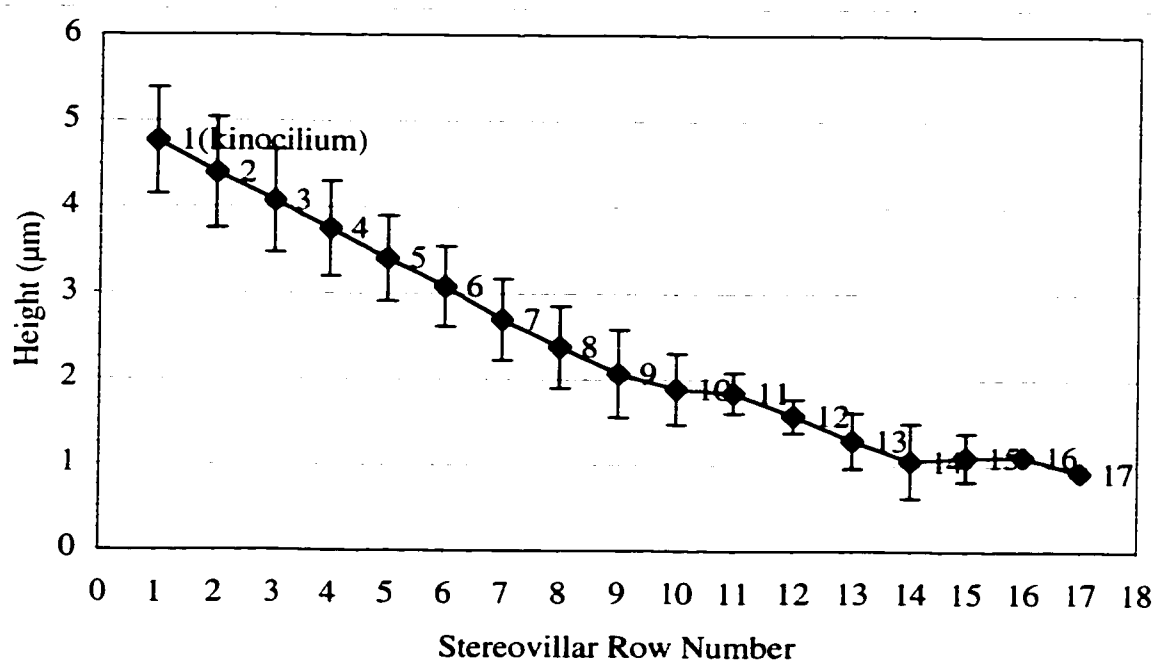

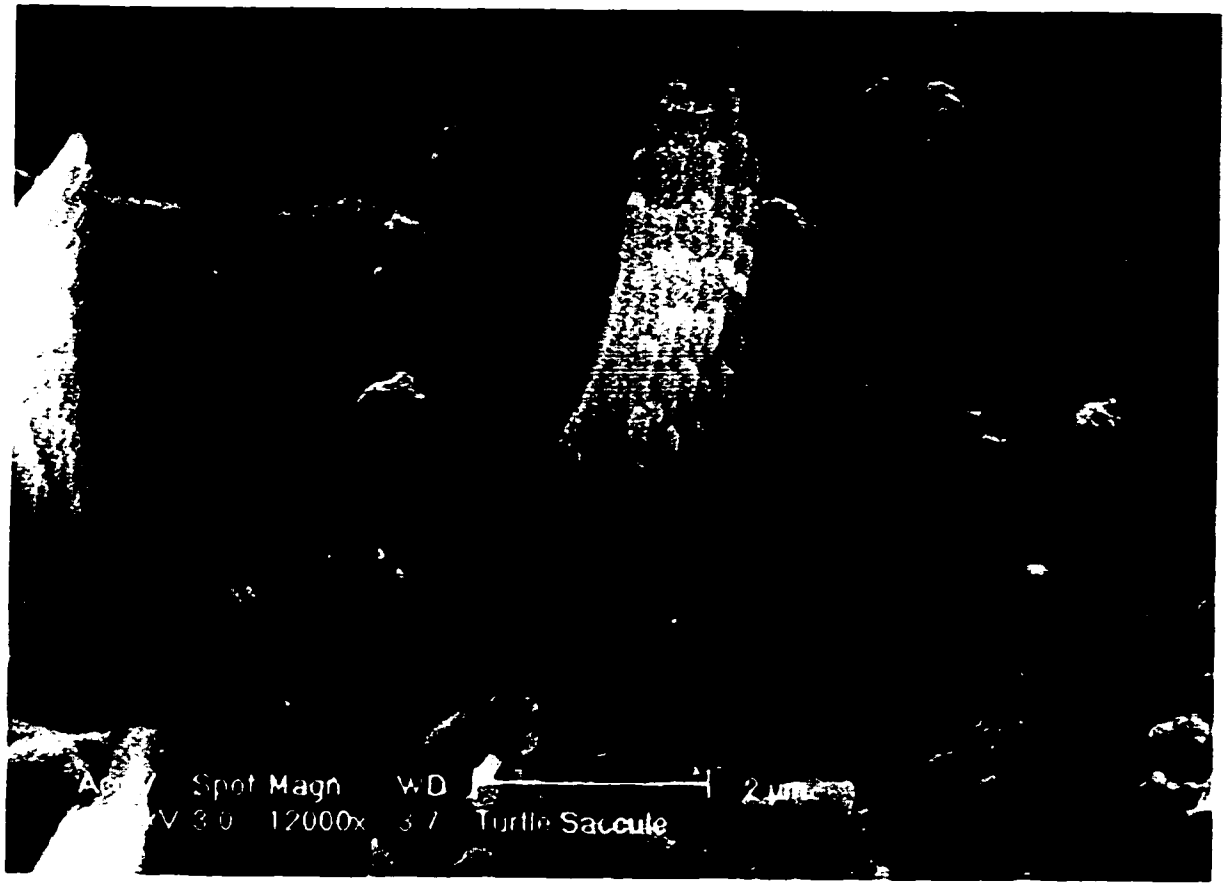


FIGURE 11. A bundle representing the typical morphology found in the striolar region. This bundle is located in the macular body. Note that the transverse stereovillar rows are closely associated (straight) such that the bundle is stereometrically tight (12000x).

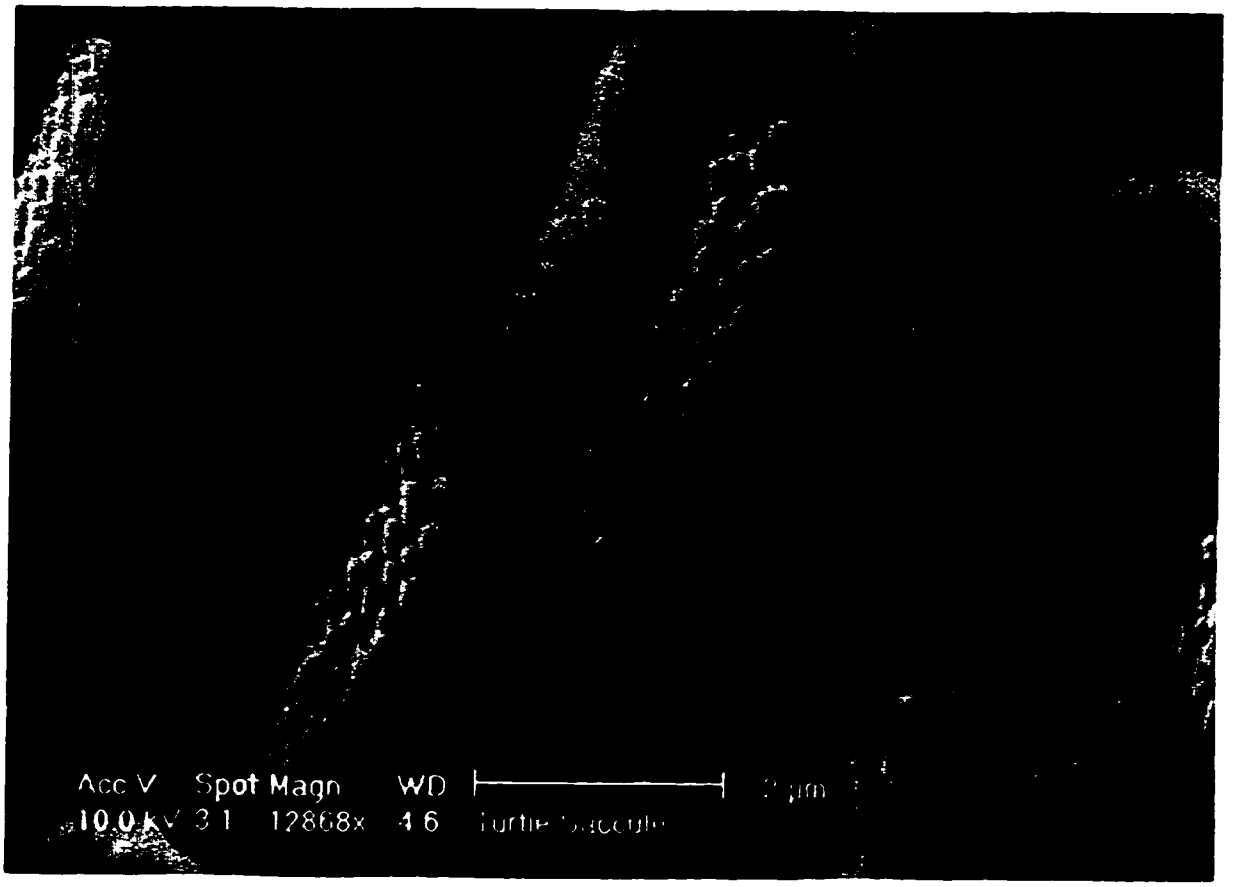


FIGURE 12. Lateral view of a bundle representing the typical morphology found in the striolar region. This bundle is located in the macular arm. Note the unimodal profile of the bundle and the small shelf formed by the first few stereovillar rows (12868x).

FIGURE 13. Kinociliar and stereovillar row numbers and heights in extrastriolar bundles (n = 9). Values are mean +/- standard deviation.

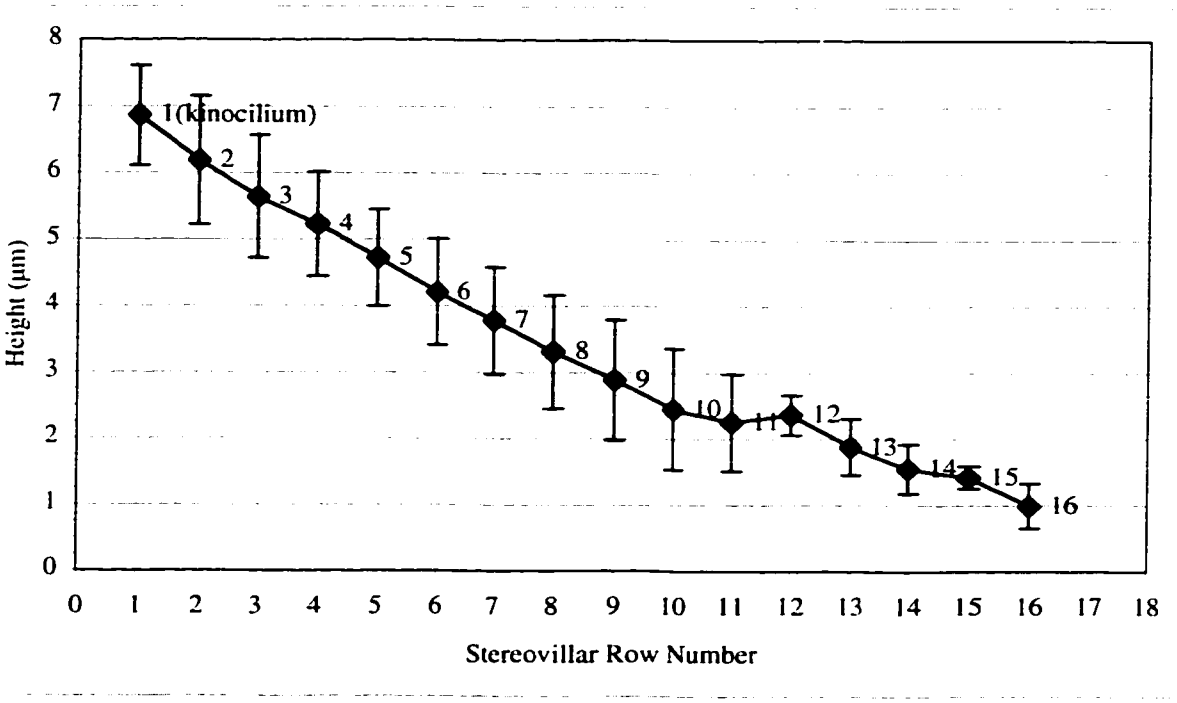

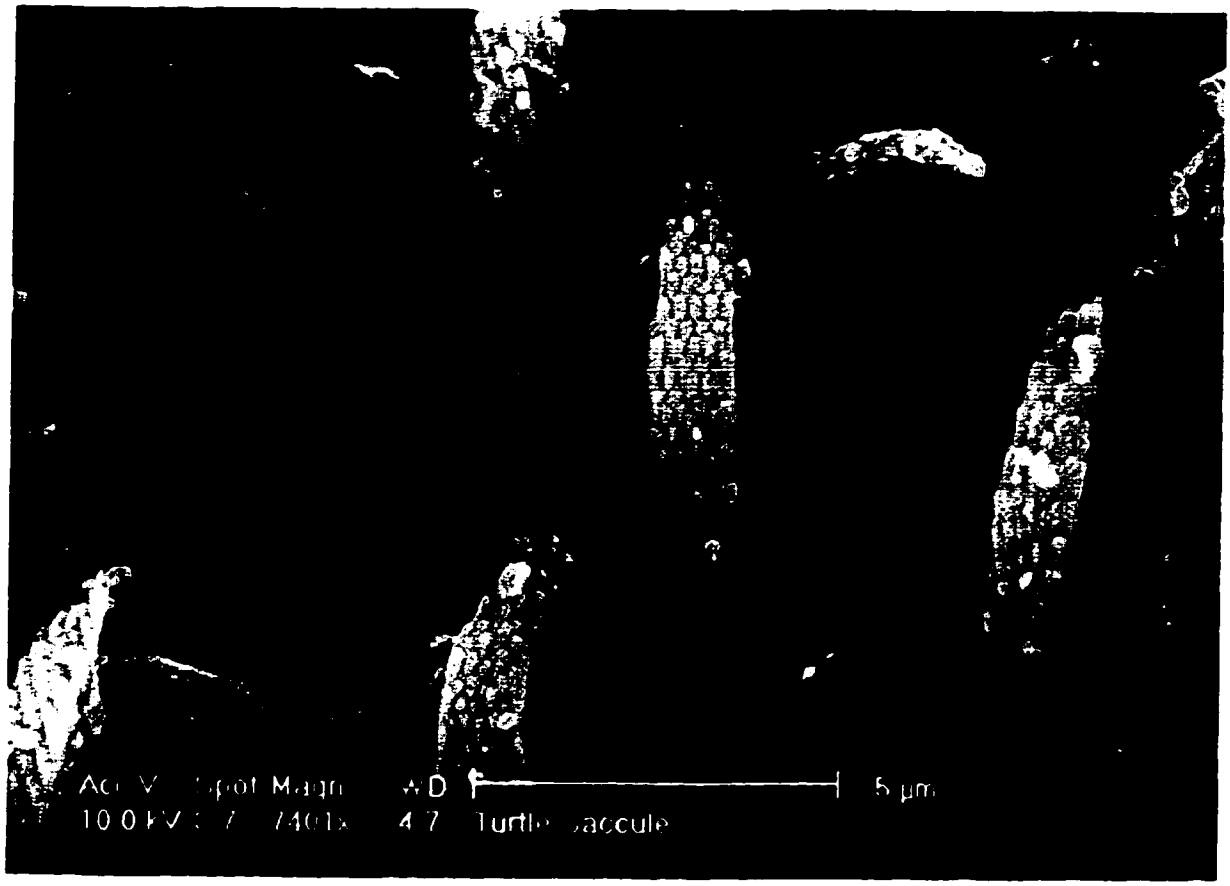


FIGURE 14. Bundles representing the typical morphology found in the extrastriolar region. These bundles are located in the macular body. Note that the bundle in the center is loose, with staggered rows, while the bundle just to the right of it is tight, with straight rows (7401x).

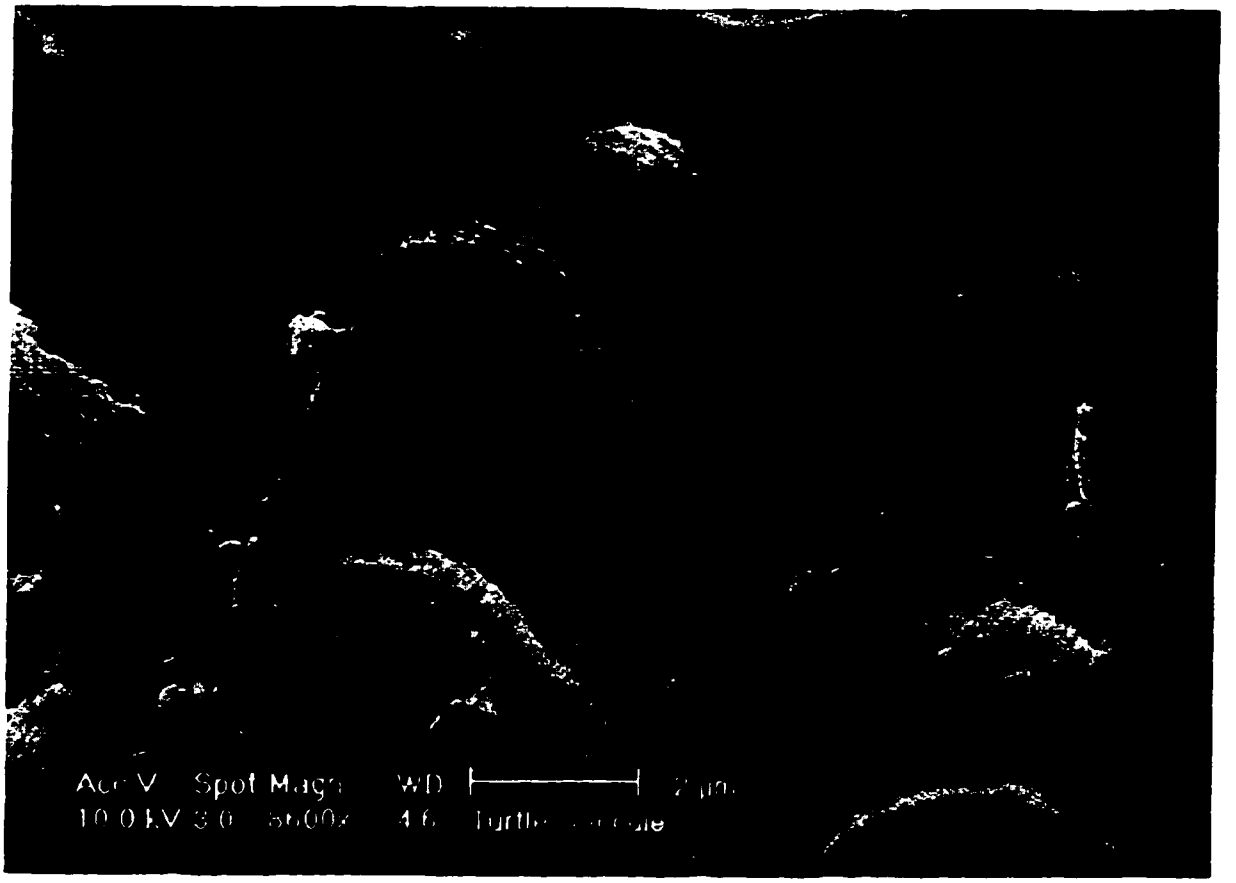

FIGURE 15. Lateral view of a bundle representing the typical morphology found in the extrastriolar region. This bundle is located in the macular arm (8600x).

FIGURE 16. Kinociliar and stereovillar row numbers and heights in peripheral bundles (n = 11). Values are mean +/- standard deviation.

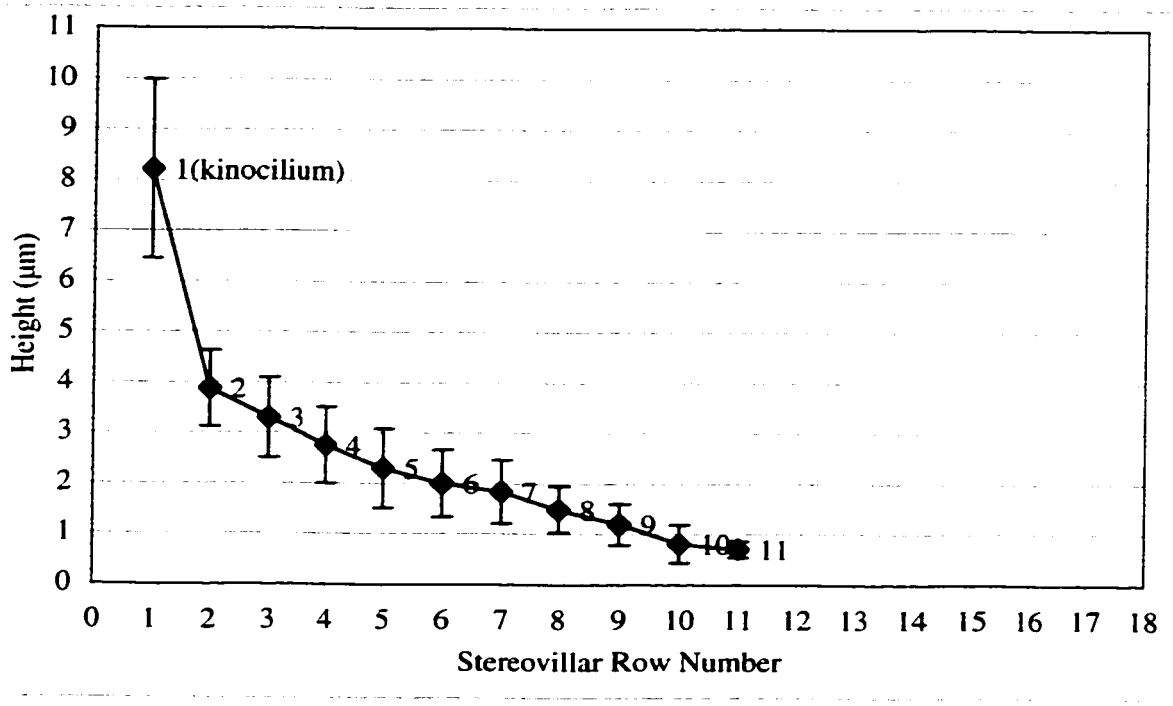

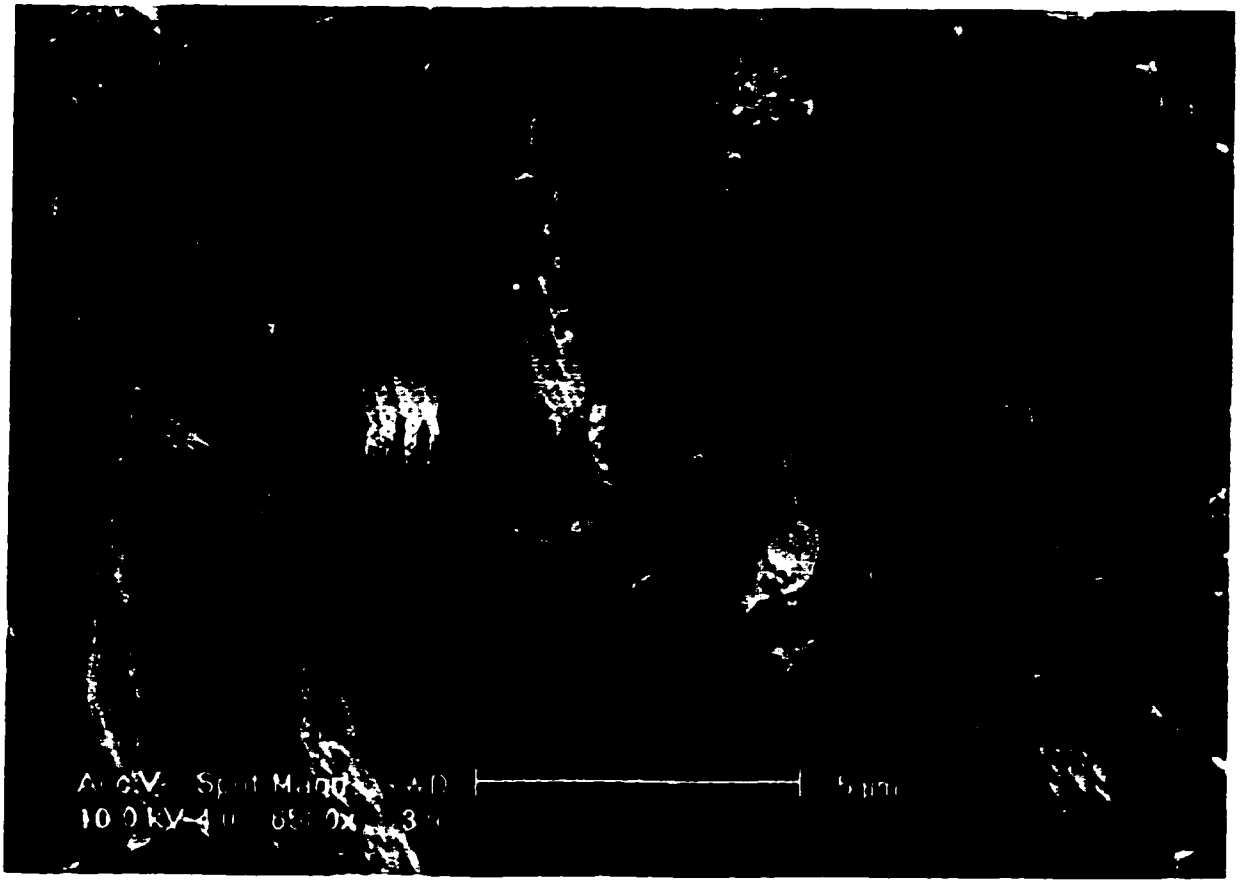

FIGURE 17. Bundles representing the morphology found in the peripheral region. These bundles are located in the macular body and are situated at the transition between extrastriolar (lower row of hair cells) and peripheral (upper row of hair cells) bundles (6580x).

FIGURE 18. Two bundles representing the morphology found in the peripheral region. These bundles are located in the macular body. Note the excessive otoconcial debris surrounding the bundles and on the tips of the long kinocilia (8509x).

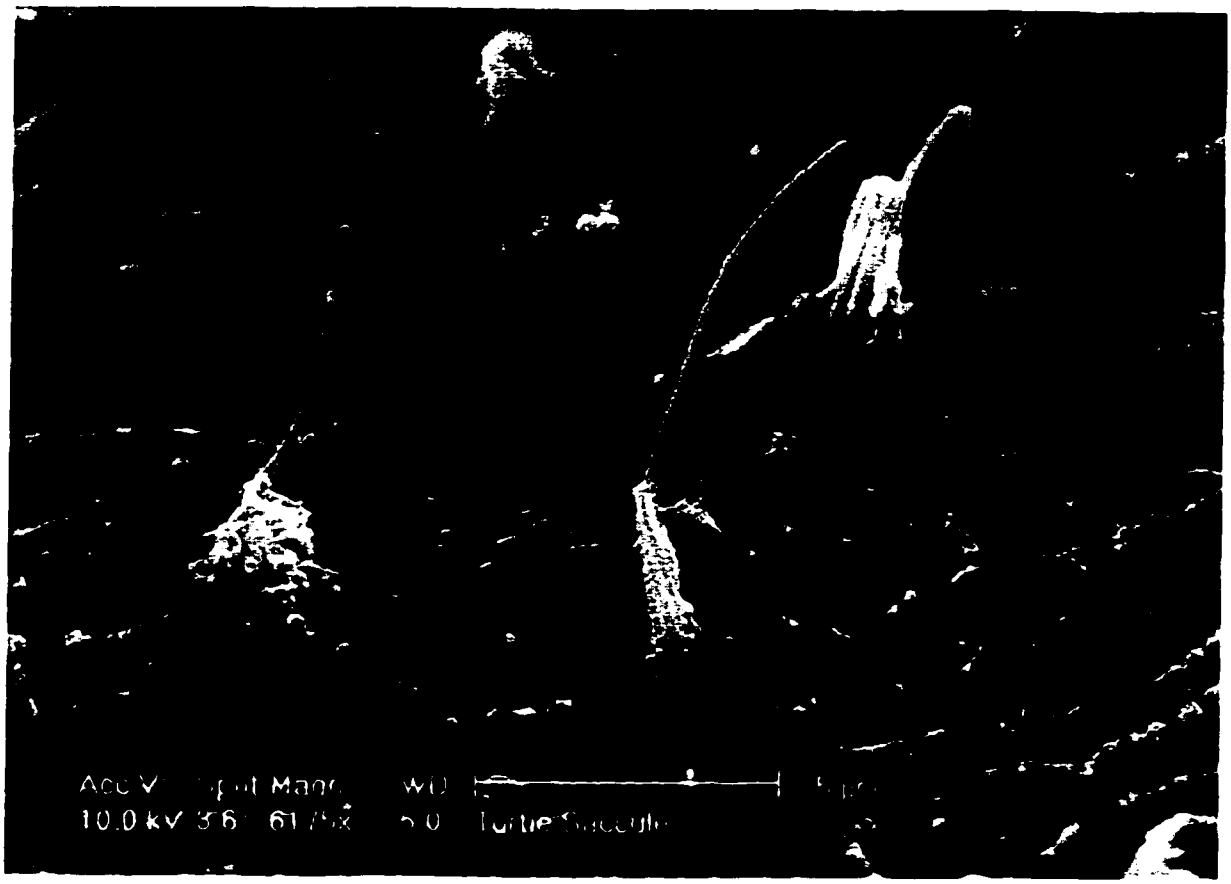

FIGURE 19. Bundles representing the morphology found in the peripheral region. These bundles are located in the macular arm and are typical of those at the extreme periphery of the macula. Note the height of the kinocilia relative the stereovilli, and the low number of stereovilli that comprise the bundles (6175x).

FIGURE 20. Scatter-plot of the number of stereovillar rows in striolar bundles with both tight (10.2 +/- 1.0) and loose (18.4 +/- 2.3) stereometric arrangements (n = 17).

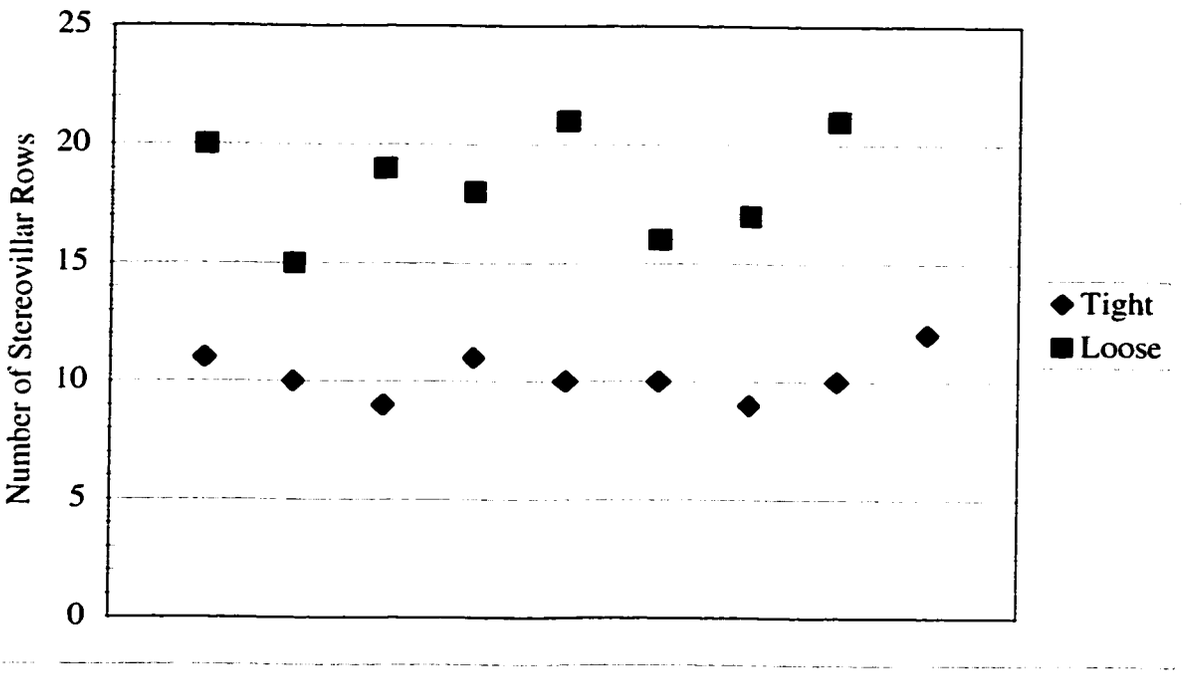

FIGURE 21. Scatter-plot of the number of stereovillar rows in extrastriolar bundles with both tight (9.5 +/- 0.7) and loose (19.7 +/- 1.8) stereometric arrangements (n = 9).

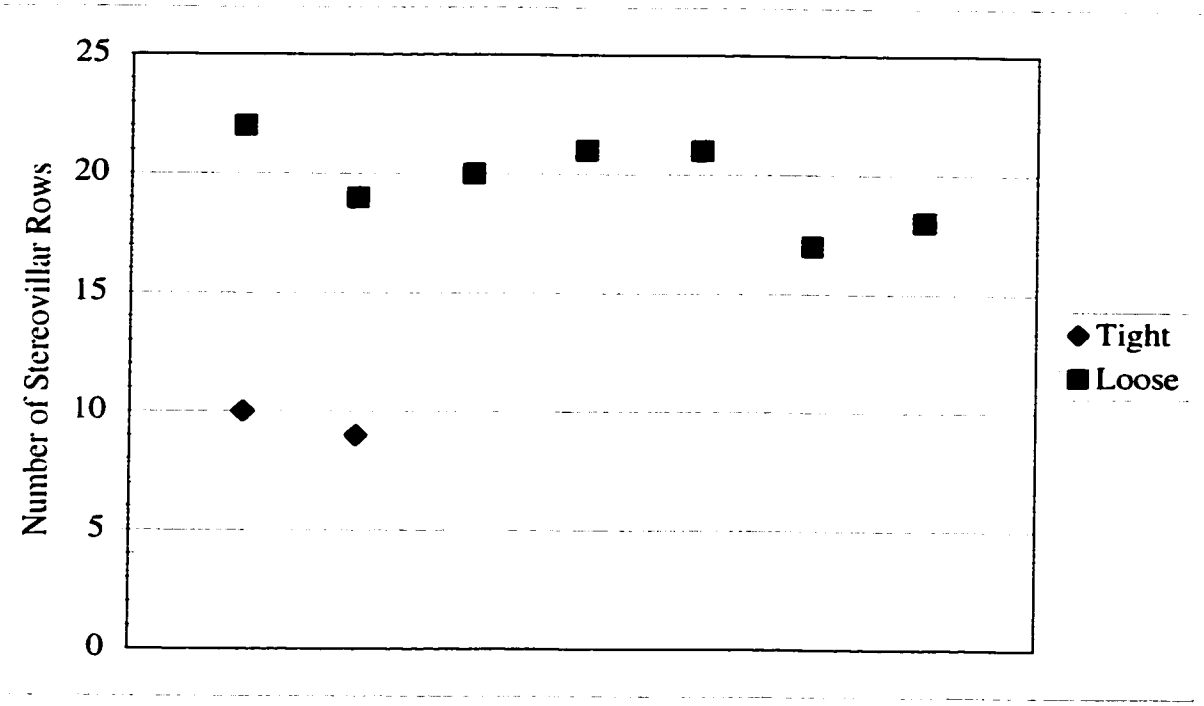

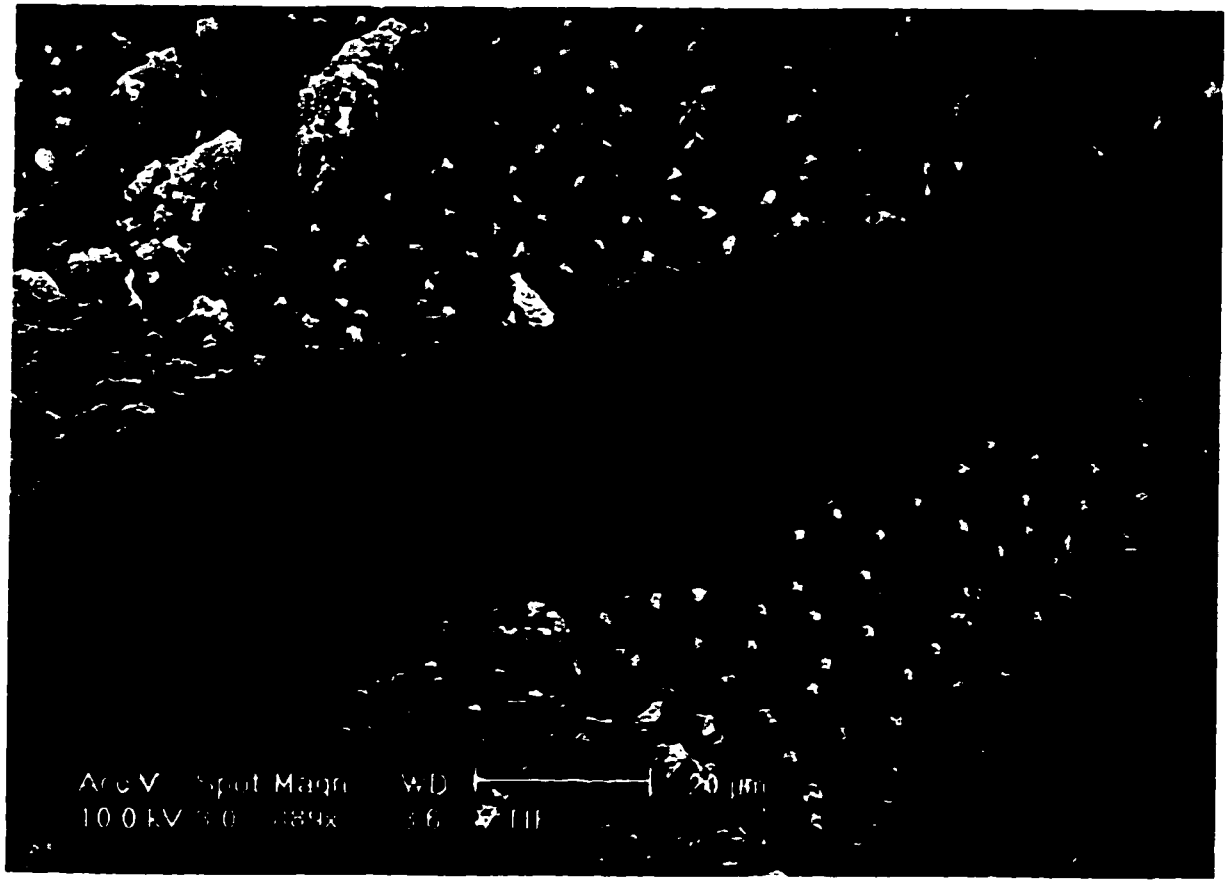

FIGURE 22. Fissure at the striola of the macular arm revealing the columnar neuroepithelium. The two visible hair cell bodies show the remnants of neural calyces. The cell bodies display flared basolateral aspects and constricted neck regions, suggesting that these cells may be type I cells. The NPRs of the cells are 0.66 and 0.60 (left to right), and the NBRs are 0.44 and 0.25 (left to right) (889x).

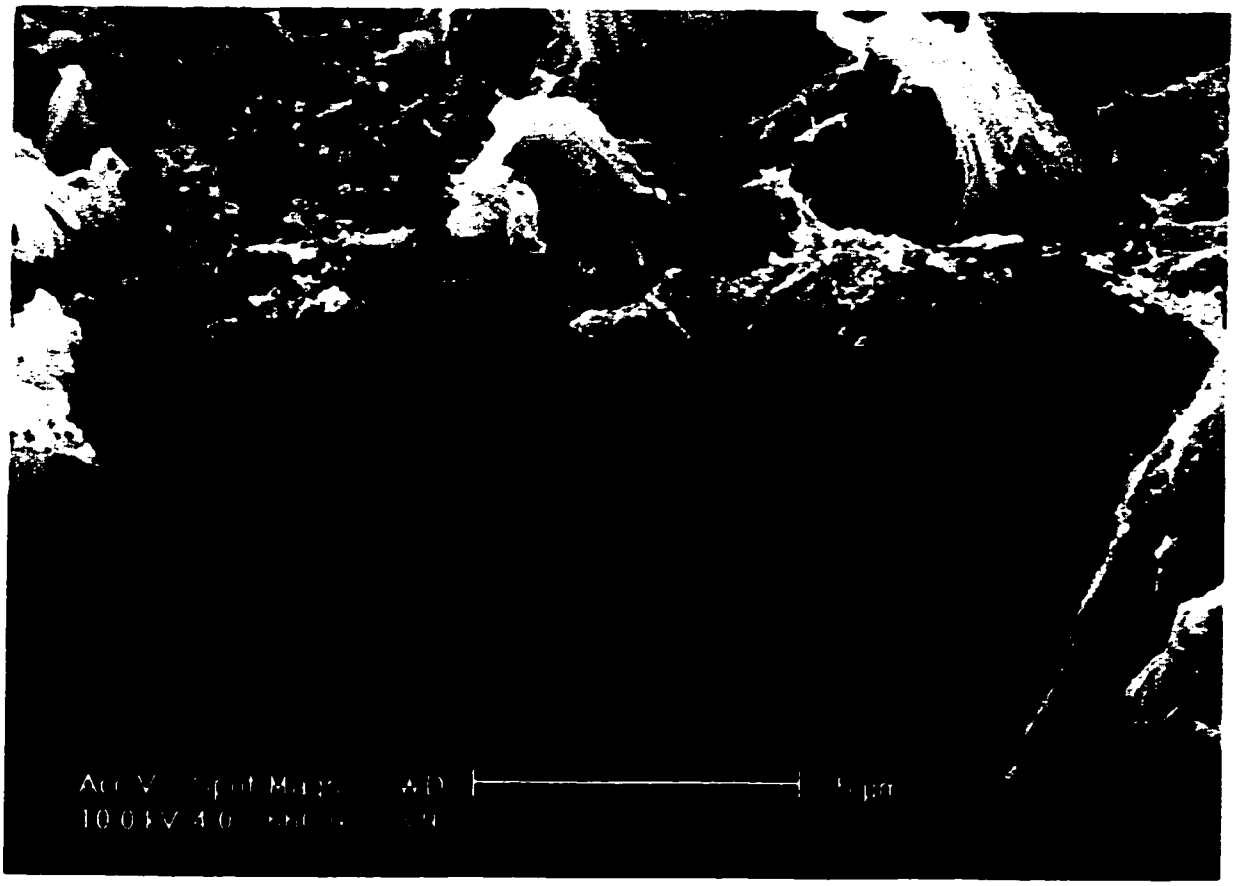

FIGURE 23. Fissure at the striola of the macular body revealing the body of a column-shaped hair cell. This shape suggests that it may be a type II cell. The NPR of the cell is 0.97 and the NBR is 0.92 (6600x).

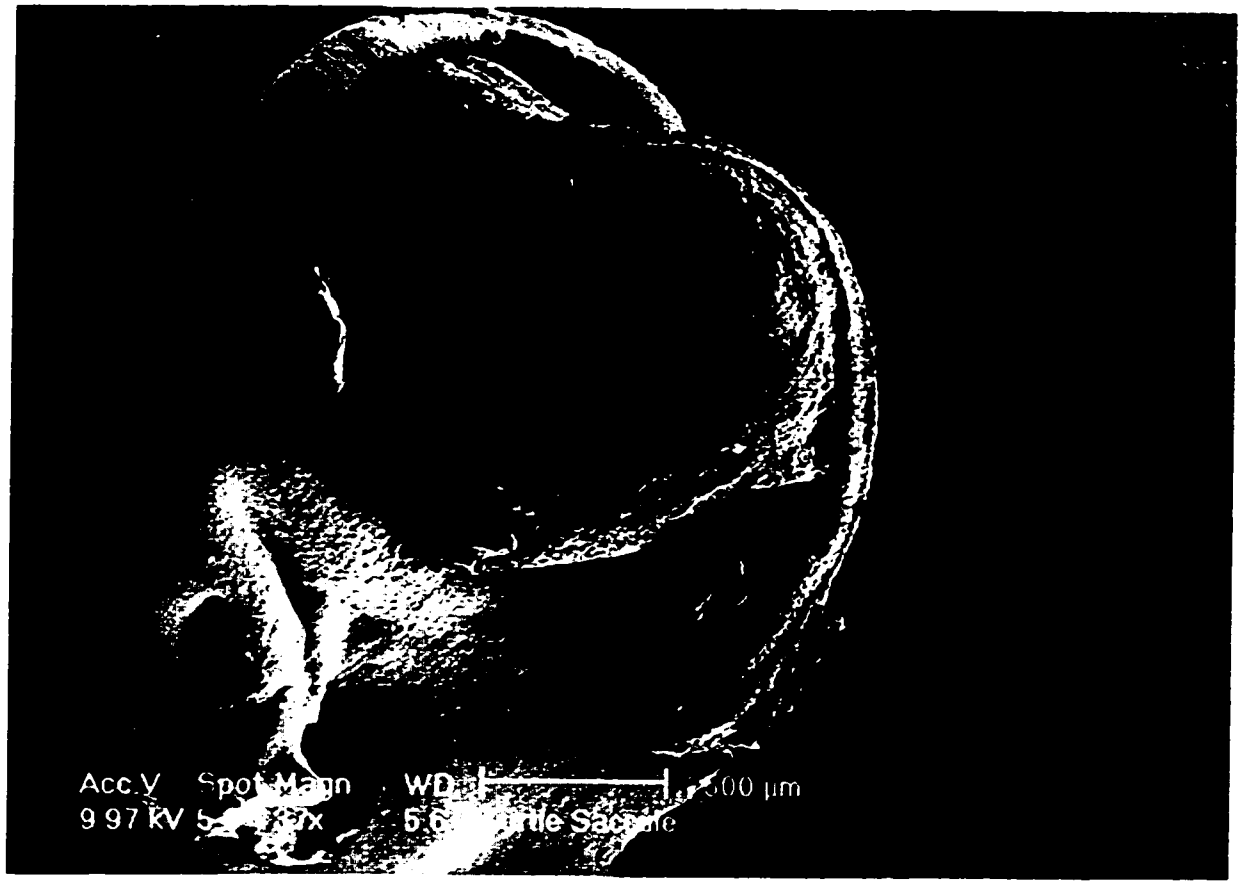


FIGURE 24. A complete otoconial mass. The mass consists of 1) a large portion that occupies most of the saccular space, and 2) a long, curved extension. The distal end of this extension is associated with the body of the macula. The proximal portion of the extension and the margin of the entire mass are associated with the macular arm. The arrows indicate the relative position of the macula in situ (37x).

FIGURE 25. Close-up of the portion of the otoconial mass that is not associated with the macula, showing the otoconia within the meshwork of the mass (1657x).

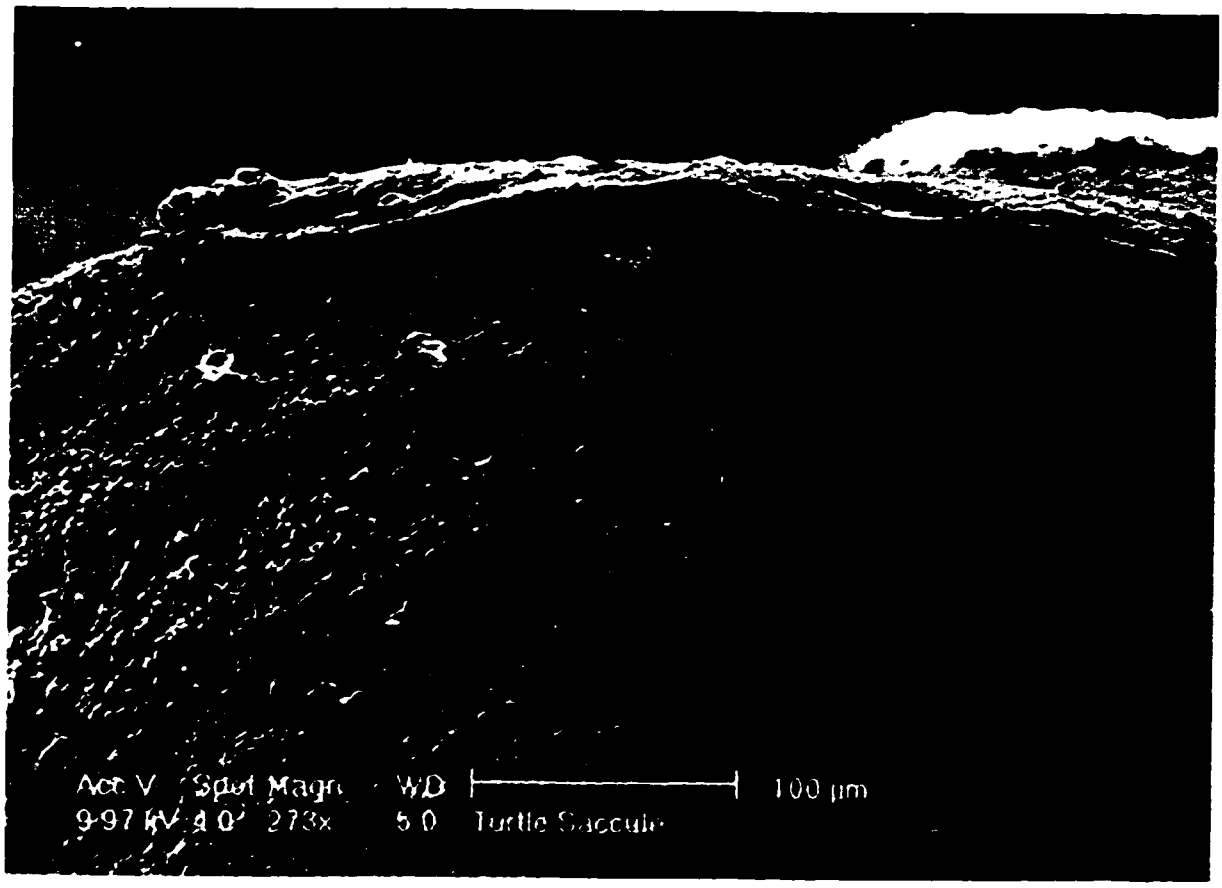


FIGURE 26. Close-up of the portion of the otoconial mass that is associated with the macula, showing the trizonal pattern. The center is approximately the width of the macular striola, and the two adjacent zones are approximately the widths of the extrastriolar and peripheral macular regions, combined (273x).

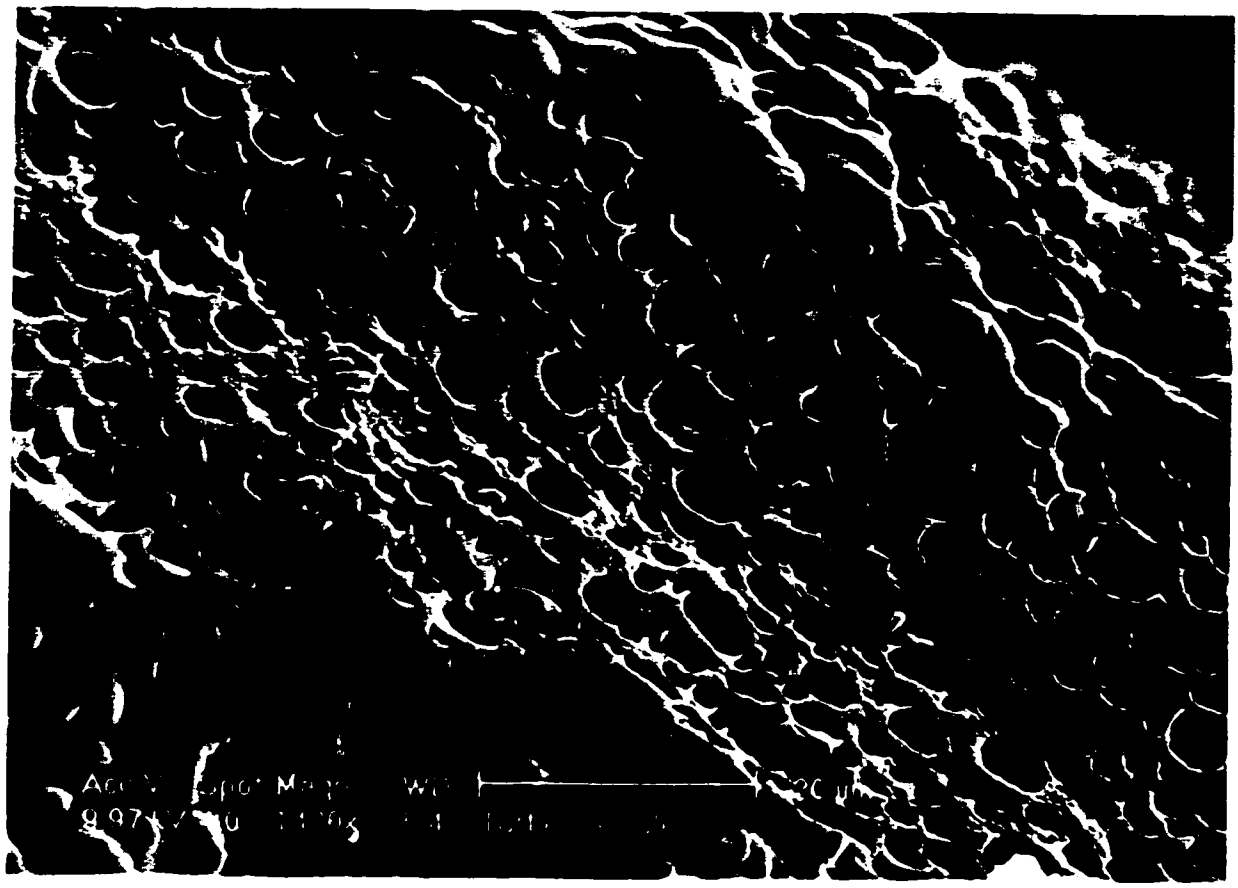

FIGURE 27. Close-up of the central portion of the otoconial mass that is likely associated with the striolar region of the macula. Note the sockets. The bundles of the striolar hair cells may be housed within these sockets (1400x).

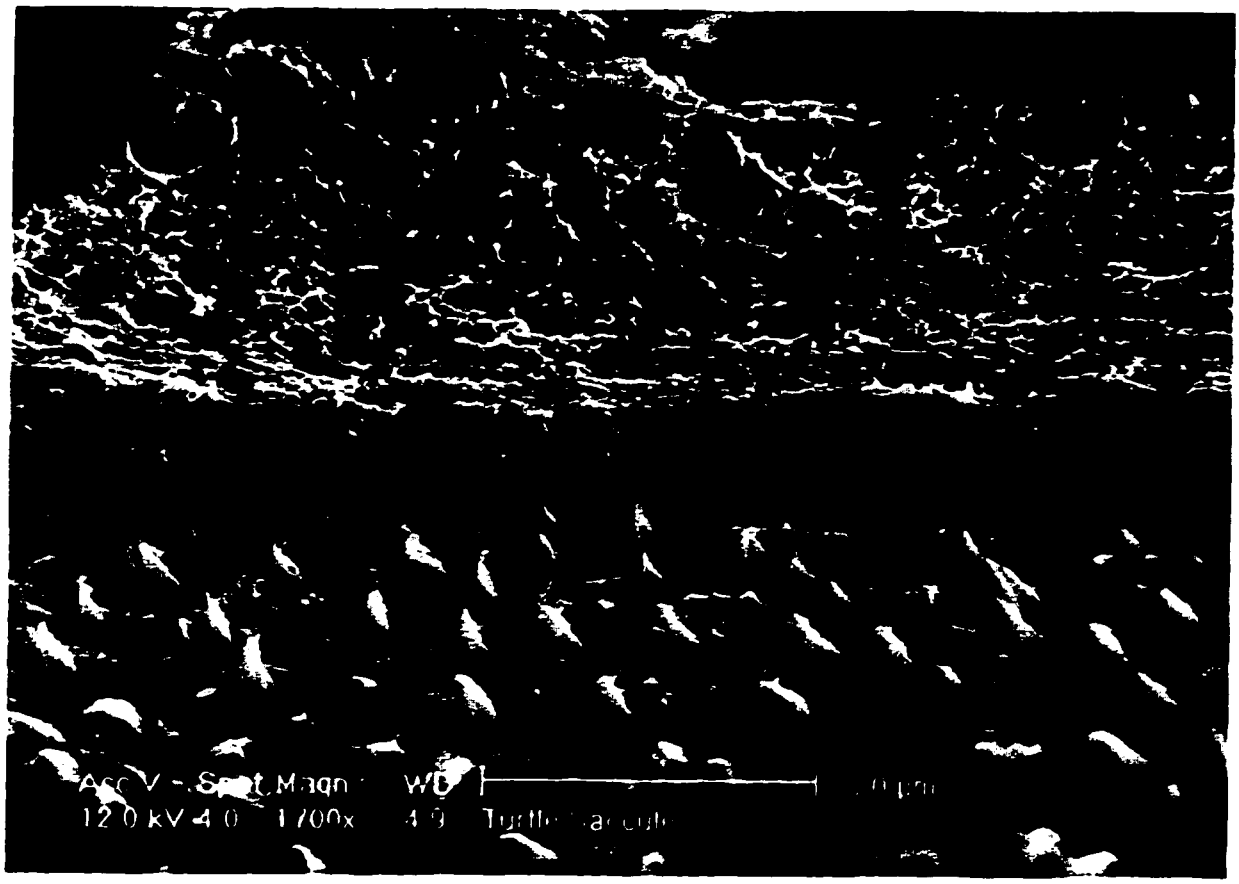

FIGURE 28. View of the otoconial membrane overlying the striolar region in the macular arm. Note the sockets within the membrane and their association with the bundles (1700x).